



THERMAL PERFORMANCE MODELING OF A DESERT HOUSE IN NEOT SEMADAR, ISRAEL



Sarah Boecker '19
Mechanical Eng.
Global Studies



Thermal Performance Modeling of Desert House in Neot Semadar, Israel

Completed abroad at the Eilat Project Center C19

A Mechanical Engineering
Major Qualifying Project submitted to the Faculty of
WORCESTER POLYTECHNIC INSTITUTE
In partial fulfillment of the requirements for the
degree of Bachelor in Science

Submitted By:
Sarah Boecker

Date:
April 2019

Report Submitted to:

Mechanical Engineering Advisor:
Isa Bar-On
Worcester Polytechnic Institute Professor

Sponsor:
Yoram Tencer
Director of Building Construction and Resident of Neot Semadar

This report represents work of a WPI undergraduate student submitted to the faculty as evidence of a degree requirement. WPI routinely publishes these reports on its web site without editorial or peer review. For more information about the project program at WPI, see <http://www.wpi.edu/Academics/Project>

Abstract

This project aimed to provide guidance to its sponsor-the construction and housing manager at a small kibbutz community in the Negev Desert in Israel-on the factors of housing construction that influence thermal performance and therefore energy efficiency of the buildings within that region. This project examined the trends that should be present in houses specific to the region based on thermal mass, insulation, glazing, directional positioning, envelope design, and the relationship between convection and radiation within the house. These trends were compared to 1) actual temperature and humidity values collected by a Worcester Polytechnic Institute Interdisciplinary Qualifying Project team in two houses on-site and 2) data collected from single-change iterations of a baseline DesignBuilder model of one of these houses created on-site. The knowledge gained from this project, written up in an approachable format, enables the sponsor to strive for informed building design and renovation in the future.

Acknowledgements

I would like to thank Worcester Polytechnic Institute and their International and Global Studies Division for making this Major Qualifying Project abroad a possibility. I would also like to thank Professor Isa Bar-On, the site-director for the Israel project site as well as the advisor of this project. Without Professor Bar-On, this project would not have been possible.

I would like to thank the following people from Neot Semadar for being so welcoming and accommodating to myself and the other students I traveled with and for making our experience as amazing as it was: Yoram Tencer, Israella, Netta, Mor, and all of the volunteers that befriended me, Jamie, Gal, Kristina, Elad, Sivan, Neer and many more.

Lastly, I would like to acknowledge the students that accompanied me on my trip to Neot Semadar and completed an Interdisciplinary Qualifying Project that aided in the conceptualization of theoretical thermal properties: Carly Whittle, Daniel Shrives, Austin Shalit and Benjamin George Tobias Stevens.

Table of Contents

Abstract.....	3
Acknowledgements.....	4
Table of Contents.....	5
Table of Figures.....	6
1 Introduction.....	8
2 Problem Statement and Project Goals.....	11
2.1 Problem Statement.....	11
2.2 Project Goals.....	12
3 Background.....	13
3.1 Mesoclimate of Neot Semadar.....	13
3.2 Bioclimatic Architecture and Thermal Comfort.....	15
3.3 Thermal Mass and Insulation.....	18
3.4 DesignBuilder v5/v6 Software.....	20
4 Iris' "Lightweight" House.....	22
4.1 Location and Geometry.....	22
4.2 House Envelope.....	24
5 DesignBuilder Model Creation.....	26
5.1 Baseline Model Inputs.....	26
5.2 Baseline Model Iterations and Results.....	40
Iteration 1: Thicker Ceiling Insulation.....	48
Iteration 2: Thicker Wall Insulation.....	50
Iteration 3: Heating System Timer.....	52
Iteration 4: Adjust Shading/Glazing.....	54
6 On-Site Data Collection.....	59
8 Future Work and Challenges.....	63
9 Conclusion.....	64
References.....	65
Appendices.....	66
Appendix A: Regional Electricity Cost by Season, Week Day, Time Part 1.....	66
Appendix B: Regional Electricity Cost by Season, Week Day, Time Part 2.....	67
Appendix C: Real Data from Light-weight house, Iris', January 30 th through February 3 rd	68
Appendix D: Real Data from High Thermal Mass house, Israella's, January 30 th through February 3 rd	69
Appendix E: Neot Semadar Weather Station Data, January 30 th through February 3 rd	70

Table of Figures

Figure 1: Neot Semadar's Art Center	8
Figure 2: Neot Semadar Average Temperatures and Daylight from the NOAA.....	14
Figure 3: Thermal Comfort Psychrometric Chart.....	16
Figure 4: Northwest facing side of Iris' house	22
Figure 5: Aerial maps of Neot Semadar showing neighborhood and house placement	23
Figure 6: Floorplan showing original structure and renovation, not as-built	24
Figure 7: New project/site dialog box screenshot.....	26
Figure 8: Neot Semadar location information, shows defaults and changes	27
Figure 9: 2D-drawing of house floorplan imported into design builder; site orientation not adjusted yet	28
Figure 10: Component Block 1 "Original House" separated into zones.....	29
Figure 11: Component Block 2: "Saferoom Extension" with one zone	30
Figure 12: Visualization with roof, prior to roof component being deleted	31
Figure 13	31
Figure 14: Iris' Original House Wall Build-Up, table to the right for readability	32
Figure 15: Iris' Original House Ceiling Build-Up, table to the right for readability	32
Figure 16: Iris' Original House Floor Build-Up, table to the right for readability	32
Figure 18: Original House Wall Properties	33
Figure 19: Original House Ceiling Properties	34
Figure 20: Original House Floor Properties.....	35
Figure 21: Construction model data for Original House block.....	35
Figure 22: Iris' Saferoom Extension Wall Build-Up, table to the right for readability	36
Figure 23: Iris' Saferoom Extension Ceiling Build-Up, table to the right for readability	36
Figure 24: Iris' Saferoom Extension Floor Build-Up, table to the right for readability.....	37
Figure 25: Saferoom Wall Properties	37
Figure 26: Saferoom Ceiling Properties	38
Figure 27: Saferoom Floor Properties.....	38
Figure 28: Construction model data for Saferoom Extension	39
Figure 29: Baseline Model Iterations.....	40
Figure 30: Baseline Winter Simulation General Criteria.....	40
Figure 31: Baseline Winter Simulation Additional Criteria	41
Figure 32: Winter Baseline Simulation Output Criteria	42
Figure 33: Five-day Graph for Non-changed Winter Simulation, Showing Temp, Heat Gains, and Energy Consumption	43
Figure 34: One-day for Non-changed Winter Simulation, Showing Temp, Heat Gains, and Energy Consumption	44
Figure 35: Five-day Graph for Non-changed Winter Simulation, Showing Comfort Properties .	45
Figure 36: Graph for Non-changed Winter Simulation, Showing Comfort Properties of Original House Structure.....	46
Figure 37: Graph for Non-changed Winter Simulation, Showing Comfort Properties of Saferoom Extension Structure	46

Figure 38: Graph for Non-Changed Simulation for Comparison to Ceiling Insulation Thickness	48
Figure 39: Graph for Original House Simulation x10 Ceiling Insulation Thickness	49
Figure 40: Graph for Non-Changed Simulation for Comparison to Wall Insulation Thickness ...	50
Figure 41: Graph for Original House Simulation x10 Wall Insulation Thickness	51
Figure 42: Graph for Original House Simulation Ceiling x10 and Wall x10 Thickness	51
Figure 43: Neot Semadar Electricity Costs by season, week day, hour, in agurot. 17% VAT not included.....	52
Figure 44: Shading Properties for Original House Structure.....	55
Figure 45: Winter Simulation with 10% glazing, comfort data.....	55
Figure 46: Winter Simulation with 60% glazing, comfort data.....	56
Figure 47: Winter Simulation with Shading	57
Figure 48: Real Data from Light-weight house, Iris', January 30th through February 3rd	60
Figure 49: Real Data from High Thermal Mass house, Israella's, January 30th through February 3rd	61

1 Introduction



Figure 1: Neot Semadar's Art Center

Neot Semadar is a modern kibbutz situated in the southern region of the Negev Desert of Israel. It is an ecological community of smart and intellectual people who welcome others from all over the world and teach them the principles of living a cooperative and creative life. Founded in 1989, it was created well after the early Zionist kibbutz movement of the 1900s that led to the settlement of land previously known as Palestine and eventually led to the creation of a Jewish state. In the 1980s, many traditional kibbutzim faced economic and ideological crises and as a result shifted to a more capitalistic and individualistic-savvy approach to their community. Many also became public entities or in some cases dissolved.

Neot Semadar was founded by a group of young Israelis in the wake of this transformation of the kibbutz and possesses a unique combination of traditional ideas and innovative approaches to their daily life-specifically centered on the idea of “self-

learning.” This means that although they are an ecological community and focus on both sustainable living and healthy human relationships with one another and nature, they also value an individual’s ability to make sense of it all and find meaning in their daily life in how *they* personally experience things.

Neot Semadar aims to teach its residents and visitors responsible citizenship, perhaps both a lingering goal of the traditional kibbutz and a concept that needs reinforcing in today’s world. Not only do they incorporate this into their daily life, with shared community support and work such as taking on laundry, preparing meals, working the crops in the field, providing childcare for one another, and taking care of and accommodating the sick but they also incorporate these values into the continuous design and improvement of their community.

One such way that they live out this value is through the design and continuous advancement of their housing. Nestled in the mountains of the Negev Desert, Neot Semadar aims to have environmentally-friendly and sustainable housing that abides by Israel’s federal desert housing standards. They do this without compromising the occupants’ personal comfort and communal preferences. With cold nights, and hot dry days throughout most of the year, it is an ideal candidate for bioclimatic architecture; “an alternative method of constructing buildings in which the local climate conditions are considered...with the aim of improving energy efficiency” (Singh, 2010).

The community at Neot Semadar has researched sustainable energy-use for years—spending 15 years designing and building their landmark art center, a “Willy Wonka-type wondrous building with a pink-and-blue tower rising above it that looks totally out of place in the area, yet magically fits perfectly,” which has been designed to

have a natural cooling tower that works passively to cool the building in tandem with the climate (Leichman, 2014). However, their theoretical knowledge has historically fallen short of their goals, as smaller cooling towers for homes failed and the art center cooling system ended up ineffective.

In this Major Qualifying Project (MQP), goals were achieved in the hopes of educating the sponsor and kibbutz members on the realities of thermal performance within their region. This project aimed to identify the most significant causes of energy inefficiency in different types of houses at Neot Semadar through thermal performance modeling and experimentation. It also enabled the creation of a guide on future building and renovation, with thermal efficiency in mind.

This project took place over the course of 8 weeks on-site at Neot Semadar as did another Worcester Polytechnic Institute project: An Interdisciplinary Qualifying Project (IQP) that collected real temperature data from various houses on-site. The IQP team of four students focused on creating a sensor that accurately measured temperature and humidity internally and externally for houses at Neot Semadar. These students assembled and tested this device on-site and aided this project in explaining the real thermal phenomena of desert housing in the winter season.

2 Problem Statement and Project Goals

2.1 Problem Statement

This project acted as a guide to explain the thermal performance of residential buildings during the mild winters and hot summers characteristic to the region of the Negev Desert in which Neot Semadar is situated. The sponsor of this project, Yoram Tencer, a director of construction at Neot Semadar, was in need of expertise in determining the most important factors in housing construction that influenced thermal performance (and therefore energy efficiency) of their buildings. The challenge of understanding what contributes to real housing conditions is not exclusive to the residents of Neot Semadar or any one type of profession: architects, engineers, construction managers, and even home owners find it difficult to understand how theoretical heat transfer principles affect the thermal comfort and performance of their homes and buildings. This project examined trends that *should* be present in houses specific to the region based on thermal mass, insulation, window-cover, directional positioning, envelope design (floor, wall, and ceiling design), and heat convection and radiation within the house. These trends were compared to *actual* recorded temperature data sets from two different types of houses at Neot Semadar as well as properties of a baseline model of one of these houses. Knowledge gained from this project enabled the sponsor to strive for more efficient and informed building design and renovation in future

endeavors. It also provided a common knowledge base from which the housing conditions at Neot Semadar could be understood and explained to its residents.

2.2 Project Goals

This project was completed on-site at Worcester Polytechnic Institute's Israel project center and involved academic work being completed both before project site arrival and during the on-site portion. Main project goals were broken down as follows:

Preparatory:

- To understand the roles that thermal mass, insulation, glazing, and positioning have on the thermal performance of a house in a desert climate
- To understand what characteristics of a building envelope, contribute to its thermal comfort and how these characteristics typically behave

On-site:

- To analyze collected temperature values for dry bulb, wet bulb, ceiling, floor, and wall temperatures in two houses at Neot Semadar: one with high thermal mass, and one light-weight and insulated
- To create a baseline model of the light-weight house
- To make single-factor changes to said baseline model to study the effects of relevant architectural choices

3 Background

3.1 Mesoclimate of Neot Semadar

Israel has a Mediterranean climate however within the country the climate varies by location despite its small size, approximately 27,000 square kilometers (a little bit larger than the state of New Jersey). Israel is split into three climatic zones with the southern-most zone being BWh according to the Köppen-Geiger classification system. BWh is a hot desert climate with an annual average temperature above 18 centigrade or 64.4° F (weatheronline.co.uk). This type of climate is characterized by 0-250 mm of rainfall annually and some of the hottest temperatures on the planet during the summer months (Britannica, 2016).

The Negev Desert itself has less than 100mm of rainfall annually in the most southern areas of the region and this small amount of precipitation is only present in the winter months (weatheronline.co.uk). When it does occur, precipitation in the area can cause erosion and flooding due to the environment not being acclimated to effects of rainfall, with loose soil and plants with narrow root systems.

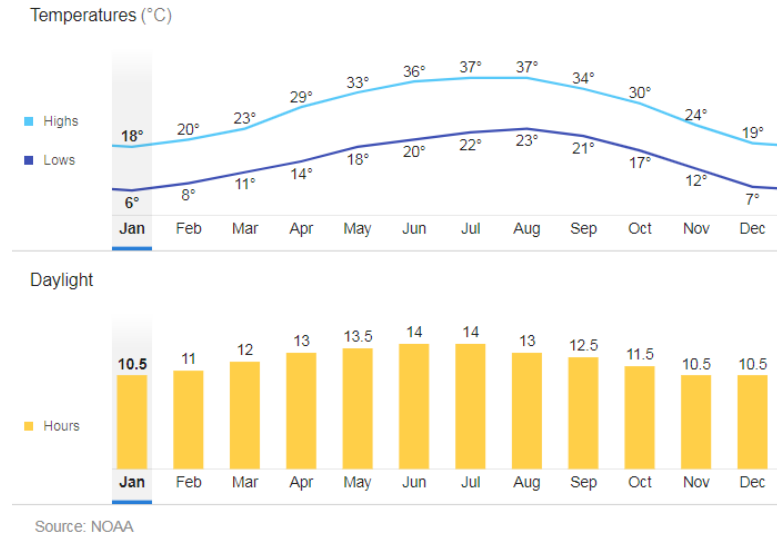


Figure 2: Neot Semadar Average Temperatures and Daylight from the NOAA

Neot Semadar has a mesoclimate that is slightly different from its surrounding desert areas. Oxford Reference defines a mesoclimate as the climate of a geographically restricted area, such as that of a forest, upland, or valley, which is not necessarily representative of the overall climate of the region as a whole. Neot Semadar, definitively fits this description due to their altitude and their unique man-made vegetation and some-1,200 trees that were planted by the kibbutz members and that are watered throughout the year. Because of this slight difference, temperatures specific to Neot Semadar, as shown in the figure above, will be used in thermal analysis and simulation instead of averages for the Negev, along with real data collected on-site. This means a high of 37 centigrade for the summer and a low of 6 centigrade for the winter will be used in order to show the extremes of both seasons in thermal simulations.

3.2 Bioclimatic Architecture and Thermal Comfort

Bioclimatic Architecture stems from a stray in mainstream architectural goals to separate and protect people from the harsh environmental conditions in which we live. It focuses more on the study of vernacular architecture or “high-comfort” living as it interacts intensely with the local environment. This field of architectural study was created by demand when environmental issues due to energy production, and therefore consumption, became clear to the public. About 60 to 70 percent of the total energy consumption in non-industrial buildings in Europe are used solely to adjust indoor temperatures to keep its inhabitants comfortable (Manzano-Agugliaro, 2015). This highlights how big of an impact passive temperature control method have on our energy-consumption as a species. We use a lot of energy to reach comfortable and healthy living conditions so harnessing the energy that exists in the climate in an area to heating advantage instead of fighting it can save a lot of money and resources. Little things such as changing the direction a house faces with respect to the sun or adding an awning that blocks solar radiation in the summer when the sun is higher than in the winter, can have a significant effect on temperature of a house.

Bioclimatic studies aim to create cost-efficient and passive systems that keep buildings at comfortable temperatures. Thermal comfort is multifaceted and is defined by both a technical component and a subjective perception component. Technically speaking, thermal comfort is based on the relationship between dry and wet bulb temperatures as well as relative humidity within an environment. However, different people have slightly different temperatures and humidity values they are most comfortable in, especially those who live in extreme climatic zones. The following graph

displays a visualization of this relationship and the complexity of determining thermal comfort when incorporating multiple factors and heating/cooling technologies.

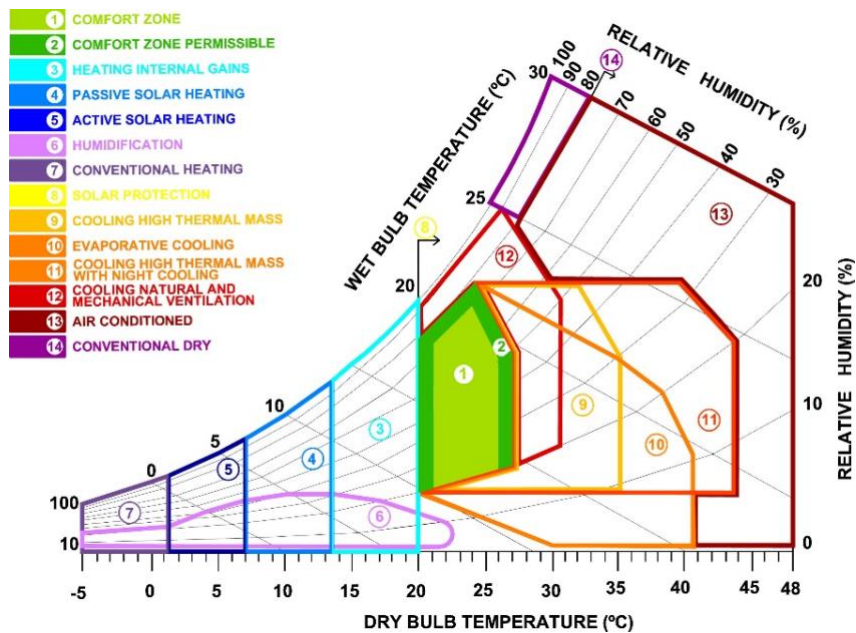


Figure 3: Thermal Comfort Psychrometric Chart

In Figure 3 above, the relationship between the dry and wet bulb temperatures and relative humidity are visualized. Wet bulb temperature is the temperature of a thermometer that is experiencing evaporative cooling at the rate that the environment allows and therefore will have a lower temperature than the dry bulb temperature. If relative humidity in an environment is 100%, then the dry and wet bulb temperatures will be the same.

It is important here to stress the difference between relative humidity and absolute humidity (the mass of water vapor in the air of a given volume). Relative humidity is the percentage of water vapor in the air as compared to the total amount of

water vapor that the air has the capacity to hold. Relative humidity is the humidity that we feel when we sit in a room. At warmer temperatures, air can hold more moisture, and at colder temperatures, the air can hold less moisture. Because of this, you can have the same mass of water in the air at two different temperatures, and at the warmer temperature the relative humidity will be lower than at the colder temperature.

The psychrometric chart in Figure 3 shows different zones of comfort in relation to temperatures and humidity. The most important zone is the comfort zone which is outlined in light green. Within this zone, 70% of people are comfortable when wearing light-clothing and remaining relatively sedentary within the space at hand. The comfort zone is characterized by temperatures around 21 centigrade to 26 centigrade and relative humidity between 20 and 70 percent. This is the ideal zone that many bioclimatic architects design spaces for. The second notable zone is the permissible comfort zone, which is displayed in Figure 3 as a darker green. This zone has slightly larger bounds than the comfort zone and 80% of people are most comfortable in this zone. As previously mentioned, comfort can be a very subjective topic, so it is important to mention that ideal comfort for individuals may vary from this chart which was created using a specific sample of people, and the comfort zone may vary in shape and size for certain populations due to their lifestyle.

In the diagram above, you may notice that in addition to the comfort and permissible comfort zones, that there are zones associated with various bioclimatic strategies. Some of these methods such as passive solar heating, solar protection, cooling high thermal mass, natural cooling and mechanical ventilation, reduced usage of high energy consuming appliances such as heaters and- more relevant to hot Israeli

summers- air conditioners. Some of these strategies can assist communities in achieving high-energy and low-cost solutions to create comfortable and healthy living environments for their inhabitants.

In order to build sustainably using these principles, a thorough understanding of the area and building at hand is imperative. Multiple climates contribute to the thermodynamics of a home: the general climate of a region, the mesoclimate, and the temperatures and wind patterns most immediately around the building (Gaitan, 2007). After this is investigated and considered within the context of the specific buildings size, shape, material, and transparency as well as external wind speeds, number of daylight hours, and even seasons, various strategies will be recommended in order to lower thermal comfort related power consumption.

3.3 Thermal Mass and Insulation

For this project, it is important to understand the composition of walls, floors, roofs and other surfaces which may affect the heat and humidity properties within a building. The properties of these different materials affect the total heat transfer through a surface based on values of thermal conductivity, emissivity, and heat transfer coefficient. These properties are at the center of thermal patterns within a home and are detailed below. A thorough understanding of these equations and properties will help in examining the outputs from the model and allow calibration of assumptions that are made. Any specific calculations made will be located in the methodology section of this paper.

1. Thermal Capacitance

$$Q = C_{th}\Delta T$$

with:

Q , energy put into the system [J]

C_{th} , thermal capacitance [$\frac{J}{^\circ C}$]

ΔT , change in temperature [$^\circ C$]

Automatic assumptions will be made in manual calculations that the energy and temperature behaviors are steady-state at given time points. The basic steady-state equations to consider within this project are:

1. Conduction

$$q'' = k \frac{\Delta T}{L}$$

with:

q'' , heat flux [$\frac{W}{m^2}$]

k , thermal conductivity [$\frac{W}{cm} \cdot K$]

2. Convection

$$q'' = h(T_s - T_\infty)$$

with:

q'' , heat flux [$\frac{W}{m^2}$]

h , heat transfer coefficient [$\frac{W}{m^2} \cdot K$]

3. Radiation

$$q'' = \epsilon\sigma T^4$$

with:

q'' , heat flux [$\frac{W}{m^2}$]

$$\varepsilon, \text{emissivity} \left[\frac{W}{m^2} \cdot K \right]$$
$$\sigma, \text{Stefan boltzman constant} = 5.67 \times 10^{-8} \frac{W}{m^2} \cdot K^4$$

These three types of heat transfer all impact systems simultaneously and make it tedious and difficult to make quick calculations to determine optimal building design or analysis. Because of this it is useful to use software to model these types of heat transfer and show the output temperatures within an environment difference or properties of materials.

3.4 DesignBuilder v5/v6 Software

One of the main features of this project is the DesignBuilder software. This is a thermal analysis simulator that allows you to build models of houses and test its heat gain, heat loss and thermal comfort throughout different times of the year at a specific location.

Some valuable inputs into the system include:

- The building position or orientation with respect to the sun
- Heating and cooling system's power, location and schedule
- Number of occupants and schedule of occupancy
- Local climate and historic weather data
- Annual to sub hourly solar angle of incidence

The system also allows for a plethora of outputs including:

- Heat loss, total and component-wise
- Heat gain, total and component-wise
- Internal temperature
- External temperature
- Comfort-level of air space within building
- All data analysis for each zone within the buildings

This software will prove useful to the methodology of this project and will be covered more extensively in the final paper, after desired features have been identified.

4 Iris' "Lightweight" House

4.1 Location and Geometry

At the time of the project, the sponsor was very interested in seeing the differences between thermal behavior and comfort within houses with higher thermal mass and houses with a lower thermal mass and more insulation. These houses with more insulation were colloquially referred to as "lightweight" houses throughout the project because they had significantly less thermal mass than others and followed more American construction conventions than typical desert structure conventions. This style of house was modeled because of its approachable geometry and floor plan as well as the successful temperature data collection within the house (covered in section 6, On-Site Data Collection) completed by the IQP students' team that were at Neot Semadar.



Figure 4: Northwest facing side of Iris' house

The specific house that was chosen for the model belonged to a kibbutznik woman named Iris. It was in the northeast section of Neot Semadar just passed their Art Center. In this area was a group of houses all constructed very similarly-if not exactly the same- to Iris' house. They each had different surrounding foliage however they were for the most part exposed equally to the sun and wind.



Figure 5: Aerial maps of Neot Semadar showing neighborhood and house placement

These houses consisted of four lightweight walls up until earlier this year when the sponsor of this project completed a saferoom renovation of each of these houses. These saferooms were made of thick concrete walls and ceilings and were designed to provide protection to the community in the event of an emergency. The floorplan in Figure 6 shows the original housing structure outlined in red and the thick concreted-walled saferoom outlines in blue. These two segments were connected during the renovation process. This floorplan was not an as-built drawing of the addition and therefore varied slightly from the floorplan used with the model creation.

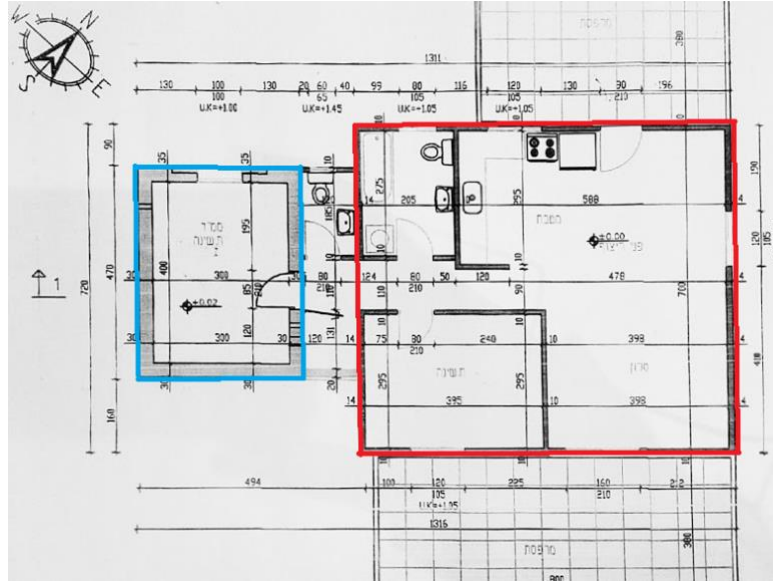


Figure 6: Floorplan showing original structure and renovation, not as-built

Figure 3 shows that the orientation of the front entrance of the house was 45 degrees to the right of the northern axis of the directional compass, which was a design choice by the builders. The house included one main living area including a kitchenette, a bedroom, a full bath within the original house boundaries, and a half bath that was included in the connection between the house and the saferoom. It also had two large overhangs on the northwest and southeast sides of the house that provided shade for those respective doors and windows as well as an outdoor seating area.

4.2 House Envelope

A house's thermal envelope is a very important property within the architectural world. Many construction codes and requirements are written in terms of their thermal envelope properties. A thermal envelope, simply put, is the 3D outline of a room or building which is bound by its ceiling floor and walls. Two main values that can

characterize the components of a thermal envelope are: 1) U Value [$W/(m^2K)$]: heat transfer coefficient and 2) R Value [$hft^2 F/Btu$]: inverse thermal resistance.

In Iris' house specifically the walls were insulated with 5 centimeters of glass wool and had a piece of drywall as the inner layer and a water-resistant drywall as the outer layer. The exact types and thicknesses of the drywalls were unknown, as well as the specific type of glass wool insulation.

The house was built on stakes creating a 20-centimeter air gap between the ground and the bottom of the house which was 6 centimeters of concrete that was layered with tiles on the top as its innermost layer.

The ceiling of the house was insulated with 10 centimeters of glass wool, with dry-wall as the innermost layer and a layer of aluminum foil on top of the glass wool. The roof covering the original building area was unoccupied and not livable. It had vents that allowed airflow through the roof structure to encourage cooling in the summer. U and R-values for the material build ups can be found in section 5.

Understanding thermal envelopes is important in order to meet the US Department of Energy IECC code – building envelope code compliance (U, n.d). This code requires specific U and R values for various components of a house and thermal envelope, and Israel desert houses must meet these requirements.

The the calculation on building envelope performance within the IECC code, describe specifically how to asses a building envelope in a real-world situation. These codes are valuable to the sponsor for future project and provide helpful background for this project.

5 DesignBuilder Model Creation

5.1 Baseline Model Inputs

This section goes through the step-by-step process through which the baseline model house was created. These steps were recommended by the DesignBuilder operation guide [insert citation reference] and enabled the correct use of the software's hierarchy structure and simulation features.

Step 1: Creation of a new site

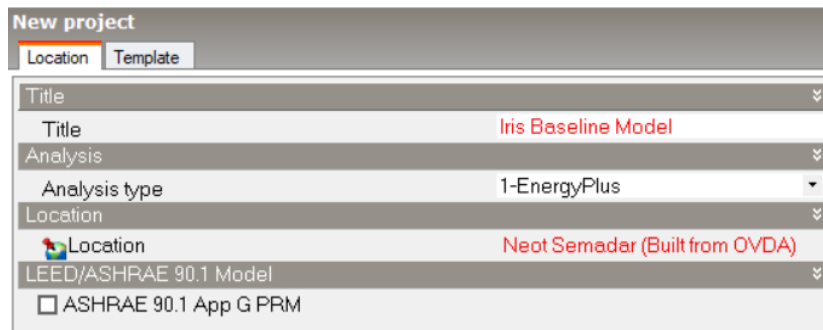


Figure 7: New project/site dialog box screenshot

In order to create a new site, a title, analysis type and location were needed. The site was named “Iris Baseline Model” and EnergyPlus was selected as the analysis type. As explained in the Background, Section 3, DesignBuilder is an interface that was created to allow easier and more approachable EnergyPlus analysis although the software can be used for other things as well.

The choice of location involved some consideration. Seasonal temperature averages and extremes used within heating and cooling system design within the software were determined based on the location chosen at this stage of the process. Simulations also pull hourly and sub-hourly weather data from the weather database associated with this location. There are a defined number of locations with weather data available in DesignBuilder with the three that are geographically closest to Neot Semadar being Ovda, Eilat, and Be'er Sheva. Eilat was determined to be too dissimilar to Neot Semadar due to its location on the Red Sea. When comparing historical weather data for Ovda and Be'er Sheva with Neot Semadar's, Ovda was the most similar. The Ovda weather station was located at the Ovda airport which was approximately 17 kilometers away from Neot Semadar.

The screenshot shows the 'Location templates' dialog box with the 'Location' tab selected. The location is 'Neot Semadar (Built from OVDA)'. The 'General' section includes fields for Country (ISRAEL), Source (ASHRAE/MSI), WMO (401980), ASHRAE climate zone (1B), Koppen classification (BWh), Latitude (30.03), Longitude (35.03), Elevation (405.0), and Standard pressure (96.2). The 'Time and Daylight Saving' section includes Time zone ((GMT+02:00) Israel), Start of Winter (Oct), End of Winter (Mar), Start of summer (Apr), and End of summer (Sep). The 'Energy Codes' section includes Legislative region (ISRAEL).

Location templates	
Location Winter design weather Summer design weather Simulation weather	
General	
Name	Neot Semadar (Built from OVDA)
Country	ISRAEL
Source	ASHRAE/MSI
WMO	401980
ASHRAE climate zone	1B
Koppen classification	BWh
Latitude (°)	30.03
Longitude (°)	35.03
Elevation (m)	405.0
Standard pressure (kPa)	96.2
Time and Daylight Saving	
Time zone	(GMT+02:00) Israel
Start of Winter	Oct
End of Winter	Mar
Start of summer	Apr
End of summer	Sep
Energy Codes	
Legislative region	ISRAEL

Figure 8: Neot Semadar location information, shows defaults and changes

Keeping this in mind, a new custom location was created for the model to represent Neot Semadar. This was built off an editable version of the Ovda site information. This location used Ovda hourly data for simulations and had the same seasonal extremes and averages as the Ovda site, however attributes such as the site Köppen-Geiger classification, location, elevation, and standard pressure were adjusted to give more accurate Neot Semadar air characteristics and sun positions/angles within simulations. Figure 5 shows default data in black and customized data for the site in red.

Step 2: Creation of new building and component blocks

Before the new building was created, a 2-D drawing of the floorplan was stripped down to included only the necessary construction lines and imported into the base plane of the model. This was rotated to have the proper site orientation which is not displayed in the figure below but is apparent in later model screenshots.

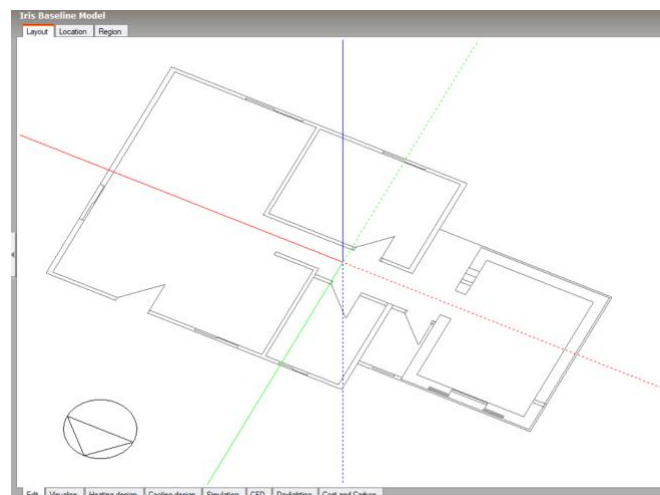


Figure 9: 2D-drawing of house floorplan imported into design builder; site orientation not adjusted yet

In order to possess the correct building geometry, the house was effectively split into two component blocks: the original house, and the saferoom. Creating these separately allowed the two different internal and external wall constructions of the sections to be assigned to each component separately.

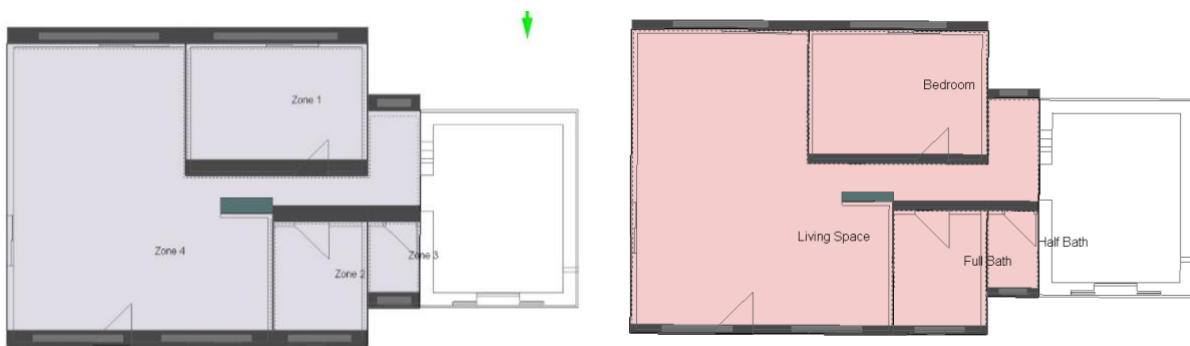


Figure 10: Component Block 1 "Original House" separated into zones

The walls drawn for blocks in DesignBuilder are external walls, so the component block boundaries snapped to meet the outermost construction lines of the 2D drawing. This block was then split into zones by drawing partitions within the block. These zones were named after their respective purposes and were given an occupancy schedule of none. This means that the software will not factor in the metabolic heat given off by human activity within the space.

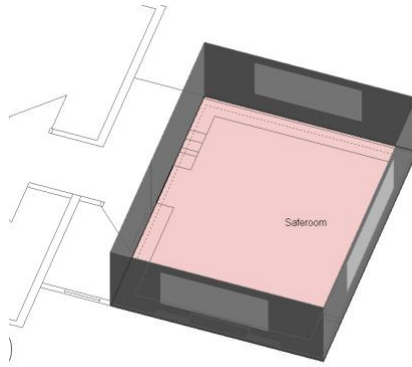


Figure 11: Component Block 2: "Saferoom Extension" with one zone

The second component block was created in the same fashion. The only difference between the two blocks was that the saferoom consisted of one zone and therefore did not require partition creation. This space was also assigned an occupancy of none.

The house under consideration also has a pitched roof covering the original structure, and flat roof on the saferoom extension. It is possible to create a component block with the correct geometry for the roof however due to time constraints and DesignBuilder considering the roof to be a second story (with the roof surface being a ceiling and the building ceiling being a floor), the roof component was removed from the simulation.

For visualization purposes, this is what the house looked like with its sloped roof:

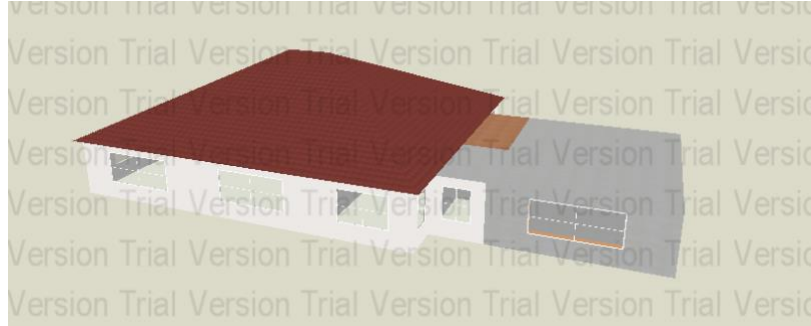


Figure 12: Visualization with roof, prior to roof component being deleted

Step 3: Set model data

As previously explained, DesignBuilder has a top-down hierarchical structure when it comes to data. All characteristics assigned at the building-level are automatically assigned to the component blocks. Because of this, the next step was to assign properties to the Original Building and the Saferoom Extensions at the block level.

For the Original Building construction, three custom materials were created that were used to define the walls, ceiling, and floor of the building. The build-ups were as follows:



Figure 14: Iris' Original House Wall Build-Up, table to the right for readability

Thickness (mm)	Material
15.80	2010 NCM Plasterboard (wallboard)
50.00	Glass fibre/wool - fibre quilt
15.80	0.625 in gypsum board



Figure 15: Iris' Original House Ceiling Build-Up, table to the right for readability

Thickness (mm)	Material
0.50	Aluminum (not to scale)
100.00	Glass fibre/wool - fibre quilt
15.80	0.625 in gypsum board

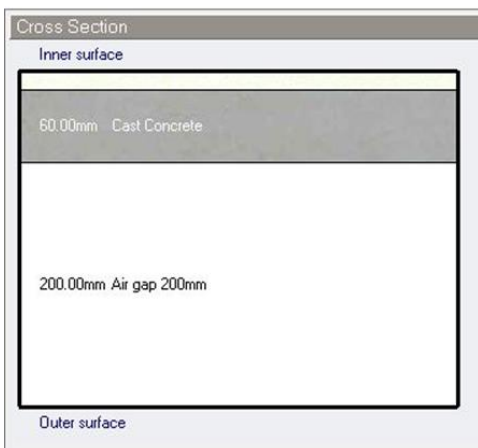


Figure 16: Iris' Original House Floor Build-Up, table to the right for readability

Thickness (mm)	Material
0.0032	Ceramic, glazed
60.00	Cast Concrete
200.00	Air gap 200mm

The basic properties for these materials are as follows, displayed in charts generated by DesignBuilder:

Constructions					
Layers	Surface properties	Image	Calculated	Cost	Condensation analysis
Inner surface					
Convective heat transfer coefficient (W/m ² -K)					2.152
Radiative heat transfer coefficient (W/m ² -K)					5.540
Surface resistance (m ² -K/W)					0.130
Outer surface					
Convective heat transfer coefficient (W/m ² -K)					19.870
Radiative heat transfer coefficient (W/m ² -K)					5.130
Surface resistance (m ² -K/W)					0.040
No Bridging					
U-Value surface to surface (W/m ² -K)					0.702
R-Value (m ² -K/W)					1.594
U-Value (W/m²-K)					0.627
With Bridging (BS EN ISO 6946)					
Thickness (m)					0.0816
Km - Internal heat capacity (kJ/m ² -K)					11.8808
Upper resistance limit (m ² -K/W)					1.594
Lower resistance limit (m ² -K/W)					1.594
U-Value surface to surface (W/m ² -K)					0.702
R-Value (m ² -K/W)					1.594
U-Value (W/m²-K)					0.627

Figure 17: Original House Wall Properties

Inner surface	
Convective heat transfer coefficient (W/m ² -K)	2.152
Radiative heat transfer coefficient (W/m ² -K)	5.540
Surface resistance (m ² -K/W)	0.130
Outer surface	
Convective heat transfer coefficient (W/m ² -K)	23.290
Radiative heat transfer coefficient (W/m ² -K)	1.710
Surface resistance (m ² -K/W)	0.040
No Bridging	
U-Value surface to surface (W/m ² -K)	0.385
R-Value (m ² -K/W)	2.769
U-Value (W/m²-K)	0.361
With Bridging (BS EN ISO 6946)	
Thickness (m)	0.1163
Km - Internal heat capacity (KJ/m ² -K)	12.4775
Upper resistance limit (m ² -K/W)	2.769
Lower resistance limit (m ² -K/W)	2.769
U-Value surface to surface (W/m ² -K)	0.385
R-Value (m ² -K/W)	2.769
U-Value (W/m²-K)	0.361

Figure 18: Original House Ceiling Properties

Constructions	
Layers	Surface properties
Inner surface	
Convective heat transfer coefficient (W/m ² -K)	0.342
Radiative heat transfer coefficient (W/m ² -K)	5.540
Surface resistance (m ² -K/W)	0.170
Outer surface	
Convective heat transfer coefficient (W/m ² -K)	19.870
Radiative heat transfer coefficient (W/m ² -K)	5.130
Surface resistance (m ² -K/W)	0.040
No Bridging	
U-Value surface to surface (W/m ² -K)	3.631
R-Value (m ² -K/W)	0.485
U-Value (W/m²-K)	2.060
With Bridging (BS EN ISO 6946)	
Thickness (m)	0.2632
Km - Internal heat capacity (KJ/m ² -K)	126.7200
Upper resistance limit (m ² -K/W)	0.485
Lower resistance limit (m ² -K/W)	0.485
U-Value surface to surface (W/m ² -K)	3.631
R-Value (m ² -K/W)	0.485
U-Value (W/m²-K)	2.060

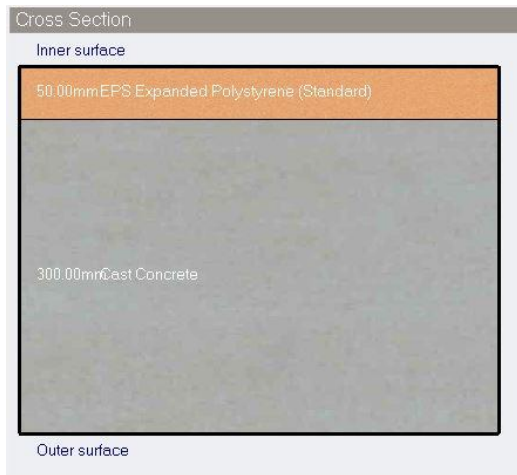
Figure 19: Original House Floor Properties

So altogether, the construction model data for the original house was as follows:

Iris Baseline Model, Building 1, Original House	
Layout	Activity
Construction	
Construction Template	
Template	Project construction template
Construction	
External walls	Iris Original House Wall
Below grade walls	Project below grade wall
Flat roof	Iris Original House Ceiling
Pitched roof (occupied)	Iris Original House Ceiling
Pitched roof (unoccupied)	Iris Original House Ceiling
Internal partitions	Iris Original House Internal Wall
Semi-Exposed	
Semi-exposed walls	Project semi-exposed wall
Semi-exposed ceiling	Project semi-exposed ceiling
Semi-exposed floor	Project semi-exposed floor
Floors	
Ground floor	Iris Original House Ground Floor
External floor	Project external floor
Internal floor	Project internal floor

Figure 20: Construction model data for Original House block

The next step was to create the wall, ceiling, and floor build-ups for the saferoom extension and to input this model data at the block level for the saferoom extension. The build ups and the overall saferoom extension construction data were as follows:



Thickness (mm)	Material
50.00	EPS Expanded Polystyrene (Standard)
300.00	Cast Concrete

Figure 21: Iris' Saferoom Extension Wall Build-Up, table to the right for readability



Thickness (mm)	Material
70.00	Cast Concrete (Lightweight)
50.00	EPS Expanded Polystyrene (Standard)
300.00	Cast Concrete

Figure 22: Iris' Saferoom Extension Ceiling Build-Up, table to the right for readability



Thickness (mm)	Material
250.00	Cast Concrete

Figure 23: Iris' Saferoom Extension Floor Build-Up, table to the right for readability

The basic properties for these materials of the saferoom are as follows, displayed in charts generated by DesignBuilder:

Inner surface	
Convective heat transfer coefficient (W/m ² -K)	0.342
Radiative heat transfer coefficient (W/m ² -K)	5.540
Surface resistance (m ² -K/W)	0.170
Outer surface	
Convective heat transfer coefficient (W/m ² -K)	19.870
Radiative heat transfer coefficient (W/m ² -K)	5.130
Surface resistance (m ² -K/W)	0.040
No Bridging	
U-Value surface to surface (W/m ² -K)	0.660
R-Value (m ² -K/W)	1.725
U-Value (W/m²-K)	0.580
With Bridging (BS EN ISO 6946)	
Thickness (m)	0.3500
Km - Internal heat capacity (kJ/m ² -K)	0.0000
Upper resistance limit (m ² -K/W)	1.725
Lower resistance limit (m ² -K/W)	1.725
U-Value surface to surface (W/m ² -K)	0.660
R-Value (m ² -K/W)	1.725
U-Value (W/m²-K)	0.580

Figure 24: Saferoom Wall Properties

Constructions					
Layers	Surface properties	Image	Calculated	Cost	Condensation analysis
Inner surface					
	Convective heat transfer coefficient (W/m ² -K)		0.342		
	Radiative heat transfer coefficient (W/m ² -K)		5.540		
	Surface resistance (m ² -KW)		0.170		
Outer surface					
	Convective heat transfer coefficient (W/m ² -K)		19.870		
	Radiative heat transfer coefficient (W/m ² -K)		5.130		
	Surface resistance (m ² -KW)		0.040		
No Bridging					
	U-Value surface to surface (W/m ² -K)		0.588		
	R-Value (m ² -KW)		1.910		
	U-Value (W/m²-K)		0.524		
With Bridging (BS EN ISO 6946)					
	Thickness (m)		0.4200		
	Km - Internal heat capacity (KJ/m ² -K)		84.6300		
	Upper resistance limit (m ² -KW)		1.910		
	Lower resistance limit (m ² -KW)		1.910		
	U-Value surface to surface (W/m ² -K)		0.588		
	R-Value (m ² -KW)		1.910		
	U-Value (W/m²-K)		0.524		

Figure 25: Saferoom Ceiling Properties

Inner surface		
	Convective heat transfer coefficient (W/m ² -K)	0.342
	Radiative heat transfer coefficient (W/m ² -K)	5.540
	Surface resistance (m ² -KW)	0.170
Outer surface		
	Convective heat transfer coefficient (W/m ² -K)	19.870
	Radiative heat transfer coefficient (W/m ² -K)	5.130
	Surface resistance (m ² -KW)	0.040
No Bridging		
	U-Value surface to surface (W/m ² -K)	4.520
	R-Value (m ² -KW)	0.431
	U-Value (W/m²-K)	2.319
With Bridging (BS EN ISO 6946)		
	Thickness (m)	0.2500
	Km - Internal heat capacity (KJ/m ² -K)	200.0000
	Upper resistance limit (m ² -KW)	0.431
	Lower resistance limit (m ² -KW)	0.431
	U-Value surface to surface (W/m ² -K)	4.520
	R-Value (m ² -KW)	0.431
	U-Value (W/m²-K)	2.319

Figure 26: Saferoom Floor Properties

Finally, the construction model data was complete, as shown in Figure 26.

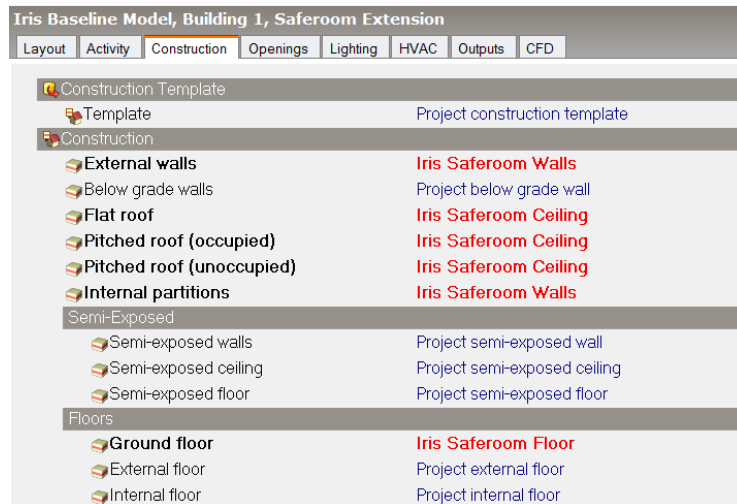


Figure 27: Construction model data for Saferoom Extension

In addition to adjusting the occupancy, and construction model data, the HVAC model data was examined at this point. When creating the building, the HVAC model data was set to <None>, and it was kept this way for each block, with the option to change it in the future. This was the completing stage of the baseline model.

5.2 Baseline Model Iterations and Results



Figure 28: Baseline Model Iterations

Figure 21, above, shows the list of single change iterations that were completed within the model. These changes were made in order to observe how these changes would affect the thermal behavior of the space within Iris' house throughout the day.

Calculation Description	
Baseline Winter Simulation	
Simulation Period	
<input type="checkbox"/> Run simulation for sizing periods	
<input checked="" type="checkbox"/> Run simulation for hourly weather	
From	
Start day	30
Start month	Jan
To	
End day	3
End month	Feb
Output Intervals for Reporting	
<input checked="" type="checkbox"/> Monthly and annual	
<input checked="" type="checkbox"/> Daily	
<input checked="" type="checkbox"/> Hourly	
<input checked="" type="checkbox"/> Sub-hourly	

Figure 29: Baseline Winter Simulation General Criteria

The settings for the simulation, as shown above in Figure 22, were the same for each iteration since the only changes were individual properties of the house. The

simulation took place over the five days of January 30th, 31st, February 1st, 2nd, and 3rd since these were the same dates over which the most reliable sensor data was collected. All output intervals were selected in order to allow for the most options for data visualization and trend observation.

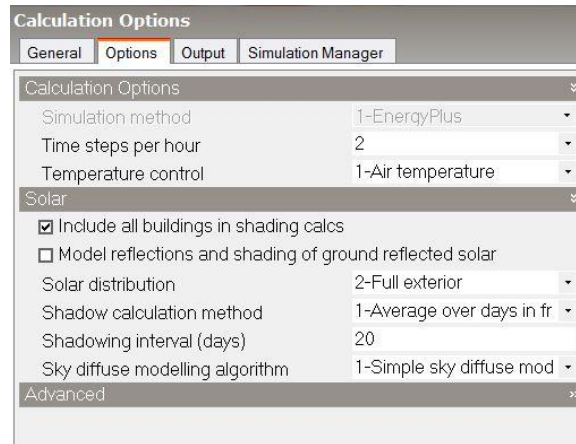


Figure 30: Baseline Winter Simulation Additional Criteria

The simulation ran at 2 steps per hour, meaning that for results displayed in sub-hourly format there were two data points saved per hour. As shown in Figure 23, above, all buildings were included in shading calculations, and all other settings were left to their default settings.

In Figure 24, below, you can see that the following output data was selected for the simulation: building and block output of zone data, unoccupied zones in block and building totals and averages (which for this project is all zones), and the custom outputs of surface heat transfer, internal gains including solar, latent loads, surface output, and opening/sub-surface output. Not all of these were plotted post-simulation but were included in order to have saved simulations with many options for data visualization.

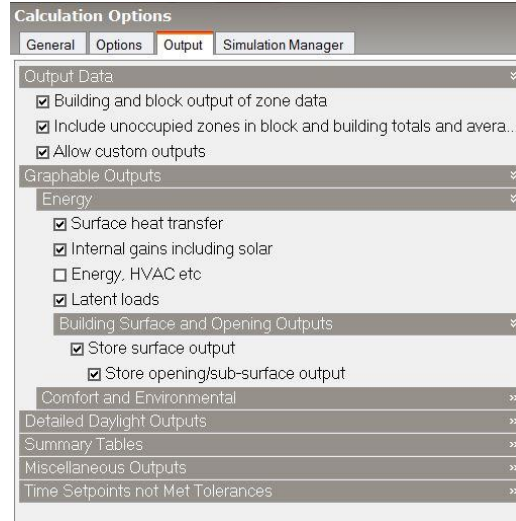


Figure 31: Winter Baseline Simulation Output Criteria

An example chart generated from a simulation can be seen below in Figure 25. The x-axis is time, with each tick mark being one full day with the chart starting at midnight on January 30th and ending at midnight on January 4th. The top row of the graph shows four temperatures throughout the day: air temperature in blue, radiant temperature, operative temperature, and outside dry-bulb temperature. You can see that on this typical winter week, it reaches around 10 centigrade at night, while a non-heated and moderately insulated house doesn't go below 13 or 14 centigrade. During the day, the outside dry-bulb temperature and the air temperature within the house peak at around 24 centigrade (about 72 Fahrenheit for comparison). In the second column, you can see the heat balance of the house (in kW). It shows all of the solar gains and losses within the environment, including glazing, walls, ground floors, partitions, exterior infiltration, solar gains exterior windows. The easiest features to see are the solar exterior window gains—the two-peaked yellow curve showing how the sun hitting

certain windows at certain times of the day affects gains—and the loss to the ground floor in brown—a pretty typical and well-known phenomenon. In many houses, the floor is the coldest surface, and this contains evidence as to why, with heat being absorbed through the floor and into the ground.

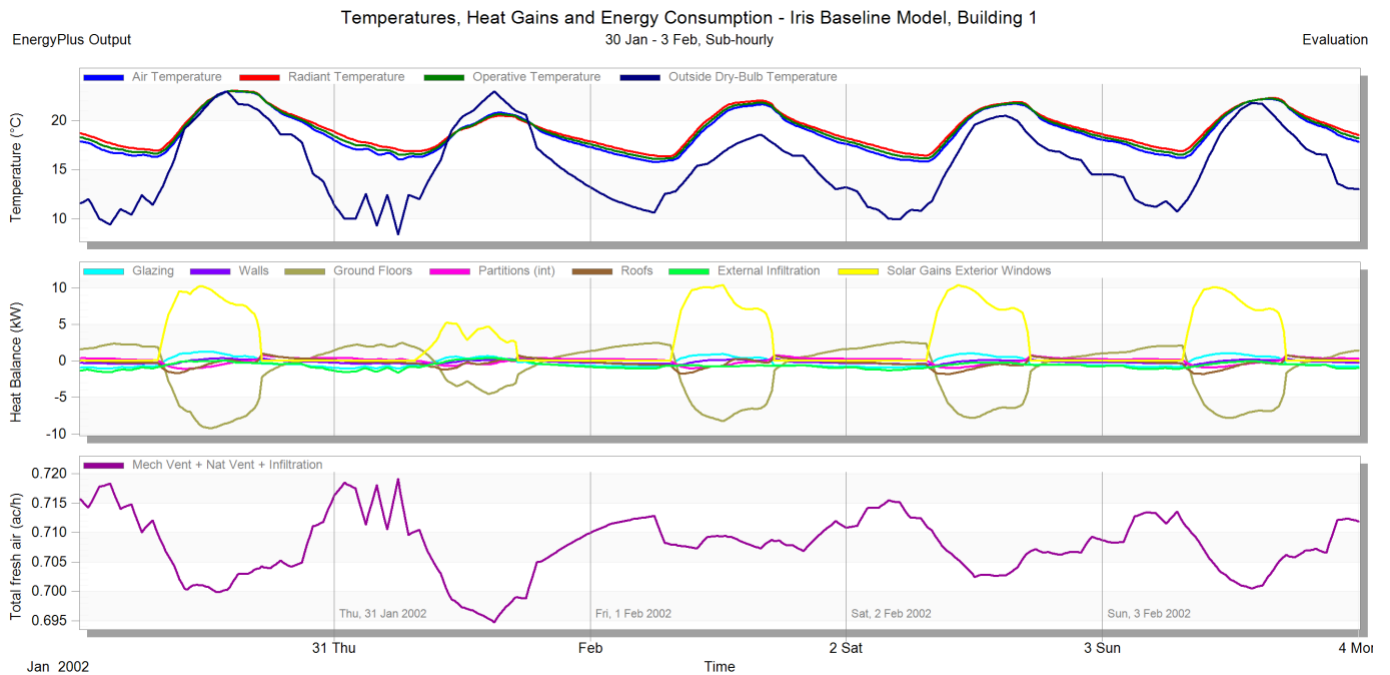


Figure 32: Five-day Graph for Non-changed Winter Simulation, Showing Temp, Heat Gains, and Energy Consumption

The third row of this chart shows the total fresh air in the house throughout the day. You can see how although data varies slightly day-to-day, the general relationship between inside and outside temperature remains constant throughout the week. Figure 26 below shows this same data but for one day, February 3rd. One can see the sub-hourly curves for gains, losses and temperatures. For this specific day you can see that the inside temperature increases slowly as the outside dry-bulb temperature increases

more rapidly, with a similar peak temperature that remains to rise for an hour or two after the outside air begins to cool.

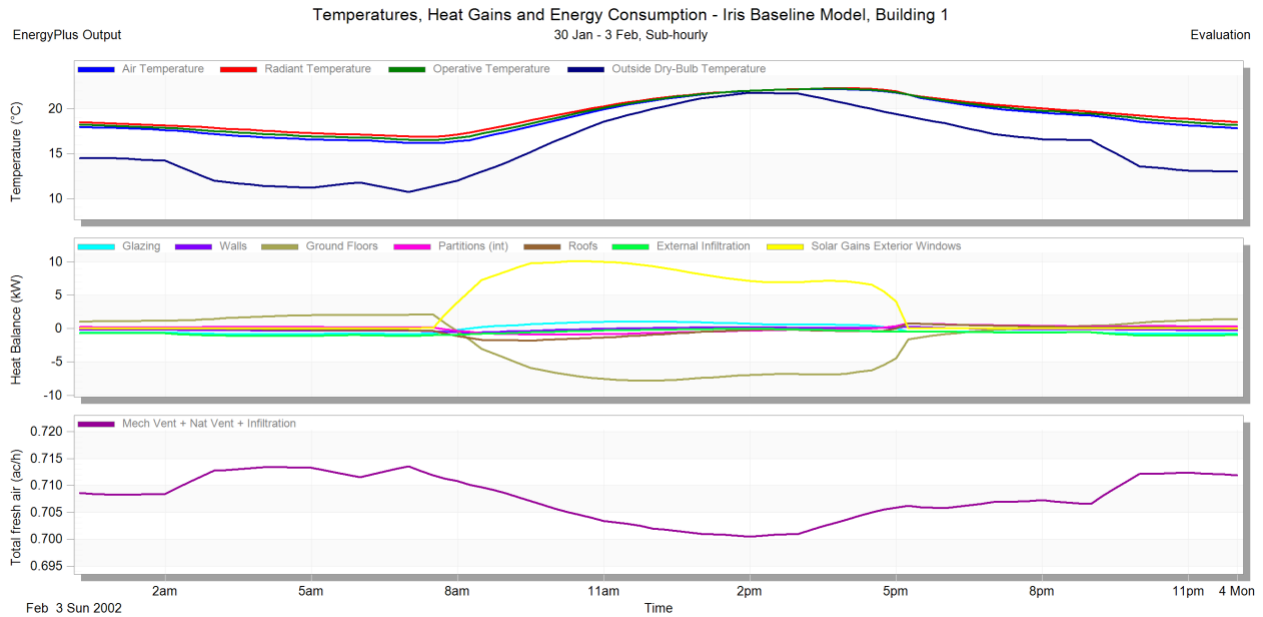


Figure 33: One-day for Non-changed Winter Simulation, Showing Temp, Heat Gains, and Energy Consumption

Figure 27 shows an alternative graph generated from the same simulation. This chart has the same top row as the previous chart; however, its bottom row displays relative humidity as a percent. The humidity and air temperature values can be plotted together to show where they lie on the bioclimatic psychrometric. Using a night time data point right before sunrise on February 1st (10.5 centigrade, 33% relative humidity) on the psychrometric chart shows that it is far outside the comfort zone and lies to the left of it in the passive solar heating zone—meaning that it would require passive solar heating to return the environment to the comfort zone.

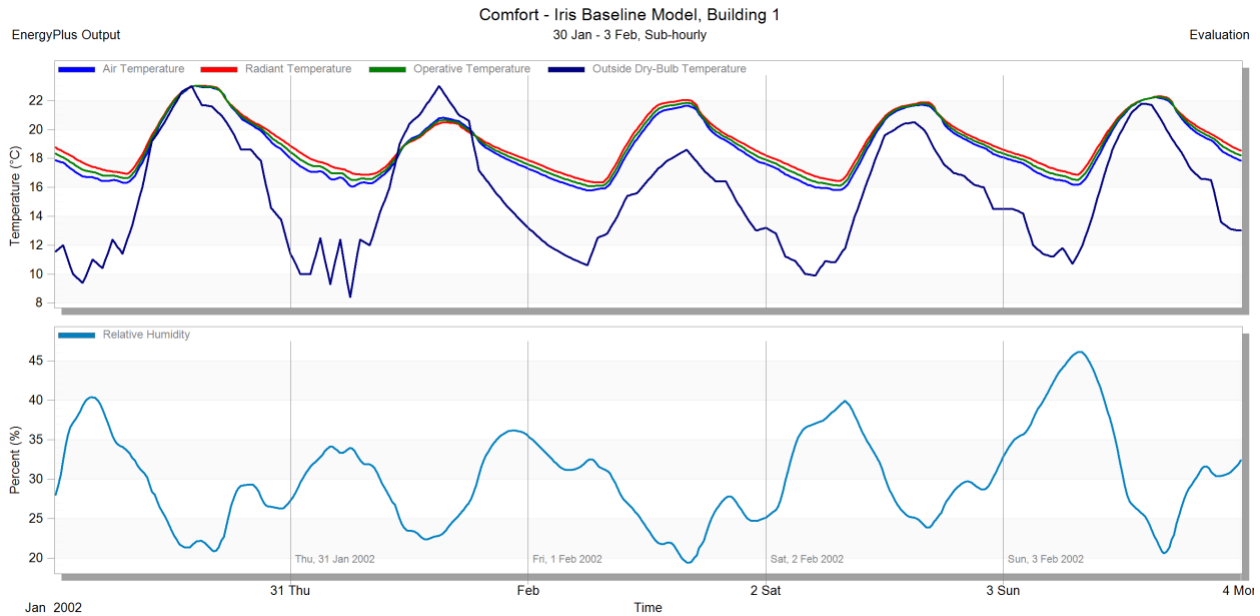


Figure 34: Five-day Graph for Non-changed Winter Simulation, Showing Comfort Properties

Using a day time data point at midday on February 1st (22 centigrade, 20% relative humidity) on the psychrometric chart will land the environment just in the comfort zone. Of course, there is variation day to day, but we can argue that according to this simulation, a typical house is inside the comfort zone during an average winter day and outside of the comfort zone at night.

Figures 28 and 29 display comfort data for just the original house structure and for just the saferoom extension structure, respectively. As covered previously, the saferoom extension is much higher in thermal mass than the original house due to its 30cm thick concrete walls and ceiling. This makes the following figure's interesting as they highlight the difference in thermal behavior between spaces with higher and lower thermal mass values.

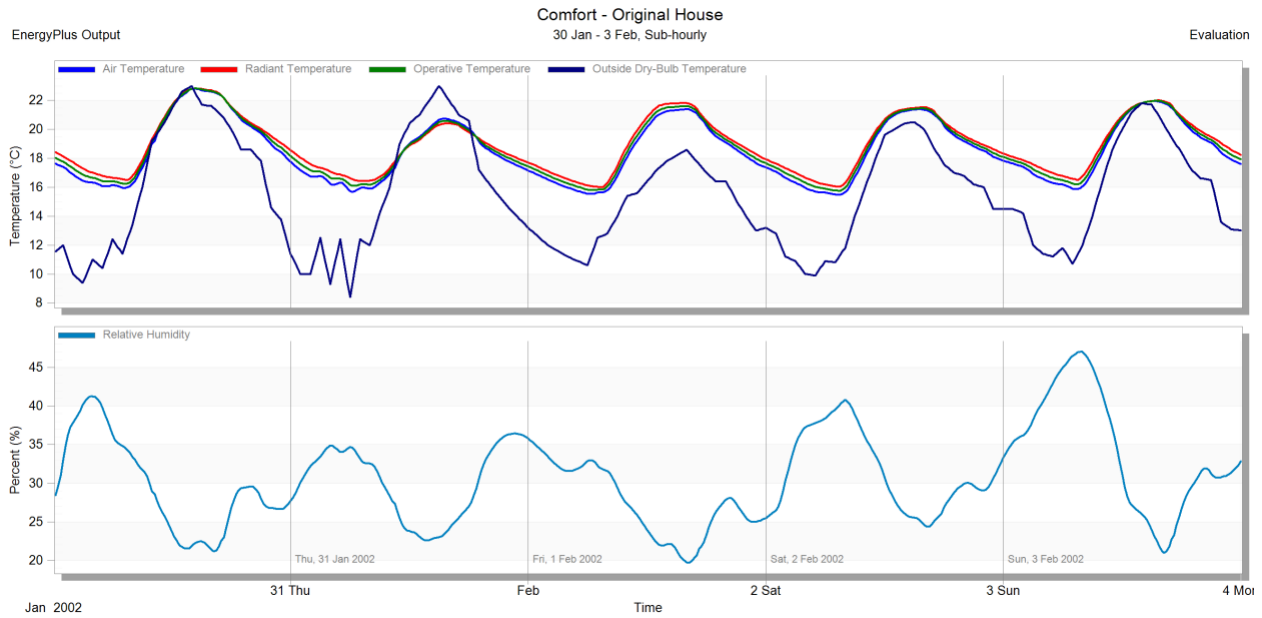


Figure 35: Graph for Non-changed Winter Simulation, Showing Comfort Properties of Original House Structure

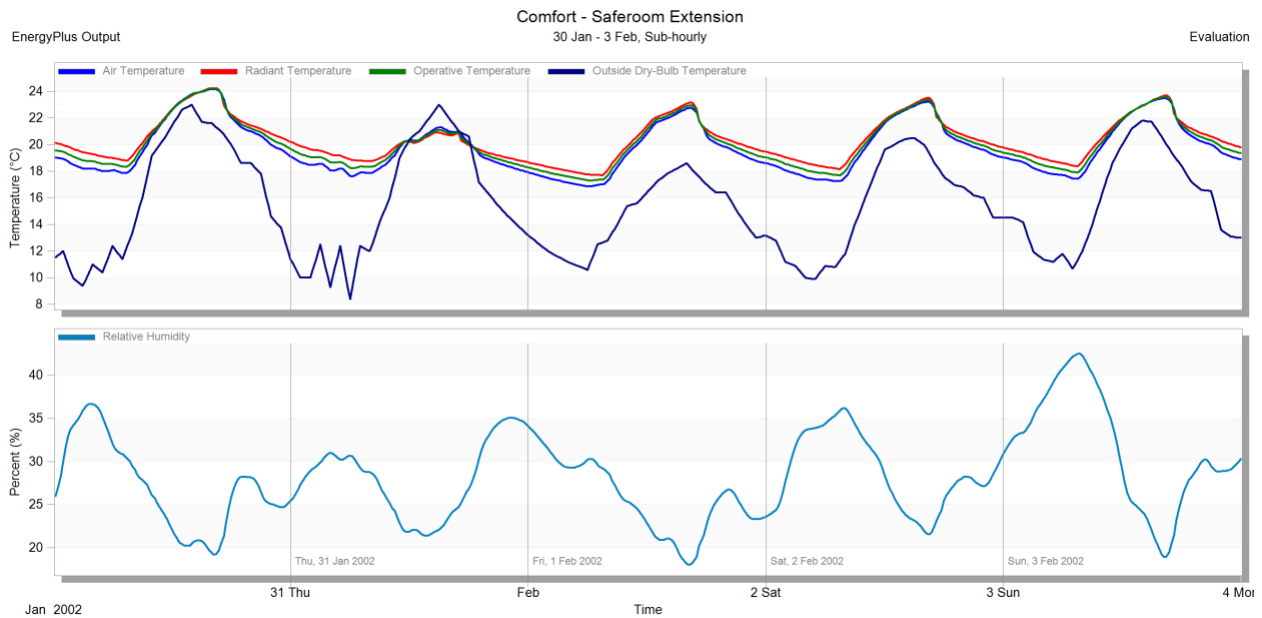


Figure 36: Graph for Non-changed Winter Simulation, Showing Comfort Properties of Saferoom Extension Structure

We can see that the shape of the curves for inside temperatures are very different for the saferoom than the original house as it heats up. The saferoom reaches a higher peak temperature but there is a time delay between that value and the peak

outside air temperature. This is due to the time it takes the high thermal mass material to absorb the heat and release it internally into the room. In the original house, a lower peak temperature is achieved but it occurs at a relatively similar time to the peak temperature outside. The peak temperature in the saferoom during the day is not within the comfort zone (plotting 24 centigrade and 19% humidity as an example data point) and falls on the line between the heating internal gains zone and the humidification zone.

One can also observe that the inside of the safe room does not cool to the same temperatures as the original house structure at night, since heat is still being radiating into the structure even after the sun has set. The initial cooling is at a faster rate due to the high difference in inside and outside temperatures, signified by the steep downward curve of the inside temperature in Figure 29, but then slows over time. The saferoom does not stay within the comfort zone at night with a sample temperature of 17 centigrade and a relative humidity of 30% at its coolest point and lies in the passive solar heating zone.

It is helpful to keep these thermal behaviors in mind as this paper examines the same graphs for different single-change iterations of the same house and system.

Iteration 1: Thicker Ceiling Insulation

The first change was to increase the thickness of insulation in the ceiling of the original house structure. Initially the insulation was 100 mm of glass wool and was doubled to 200 mm to run the simulation. The change in behavioral properties was so miniscule that another simulation was run with x10 glass wool insulation, 1000 mm or 1 meter, in order to better display the change in thermal properties.

Figure 30 below, is the same as Figure 28, and shows the general thermal behavior of for five days within the original house structure, and Figure 31 shows the same information but with an increased ceiling thickness of x10.

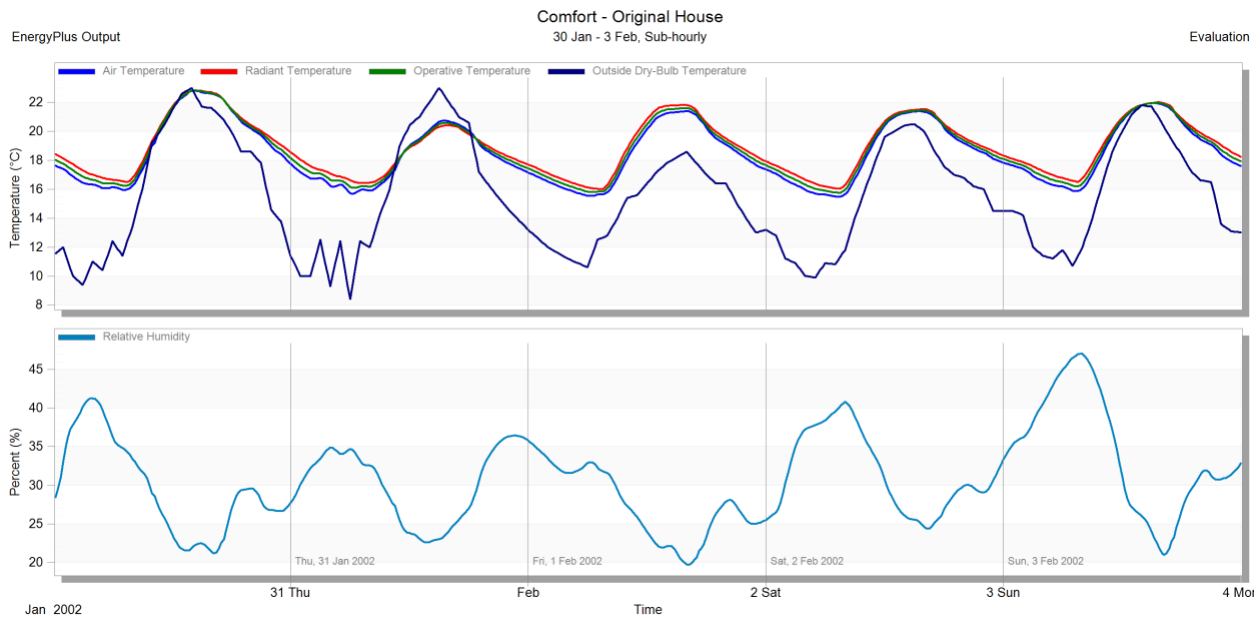


Figure 37: Graph for Non-Changed Simulation for Comparison to Ceiling Insulation Thickness

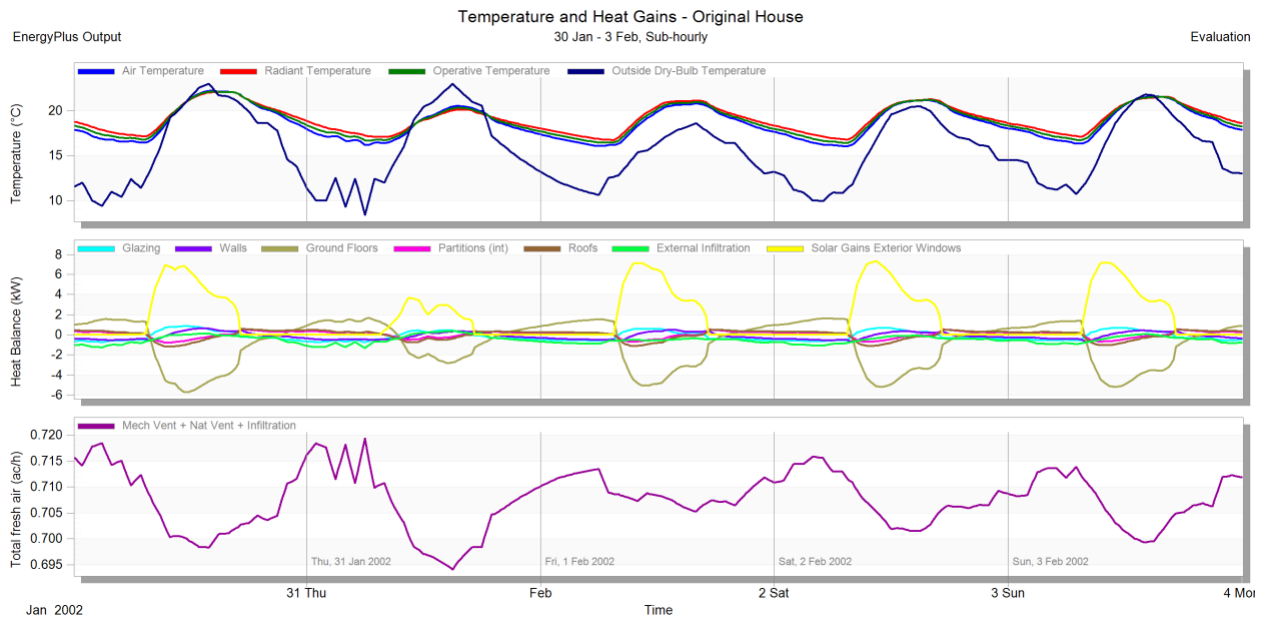


Figure 38: Graph for Original House Simulation x10 Ceiling Insulation Thickness

You can see that in the graph with the thicker ceiling insulation that the inside air temperature peak is slightly lower, easily shown by the outside dry-bulb peak temperature on January 30th being higher than the inside temperature.

Iteration 2: Thicker Wall Insulation

The second iteration was to change the thickness of insulation in the wall. The original thickness was 50 mm of glass wool and was increased to 100 mm in the simulation. Similarly, to the ceiling insulation iteration, the change in thermal behavior was not drastic enough to be visible in the data visual. In order to display the effects more clearly, the insulation was increased to 500mm or 0.5 m, a factor of 10. The difference in thermal behavior can be seen by examining Figures 32 and 33

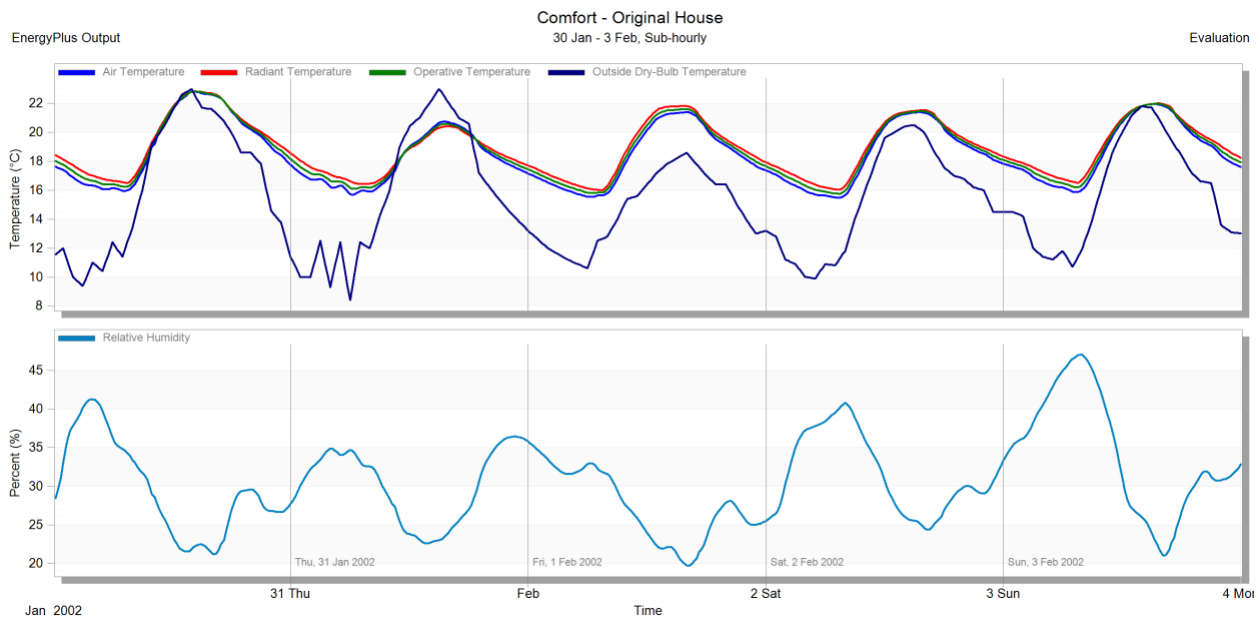


Figure 39: Graph for Non-Changed Simulation for Comparison to Wall Insulation Thickness

A similar phenomenon can be observed for the increased wall insulation thickness, where the inside air temperature does not reach the same peak, and also remains slightly warmer at night, by about one or two degrees. This shows that the heat

absorbed during the day is radiated into the space during the day. This amount of increased insulation has a regulating effect where the peak temperature is not as high and the lowest temperature is not quite as low.

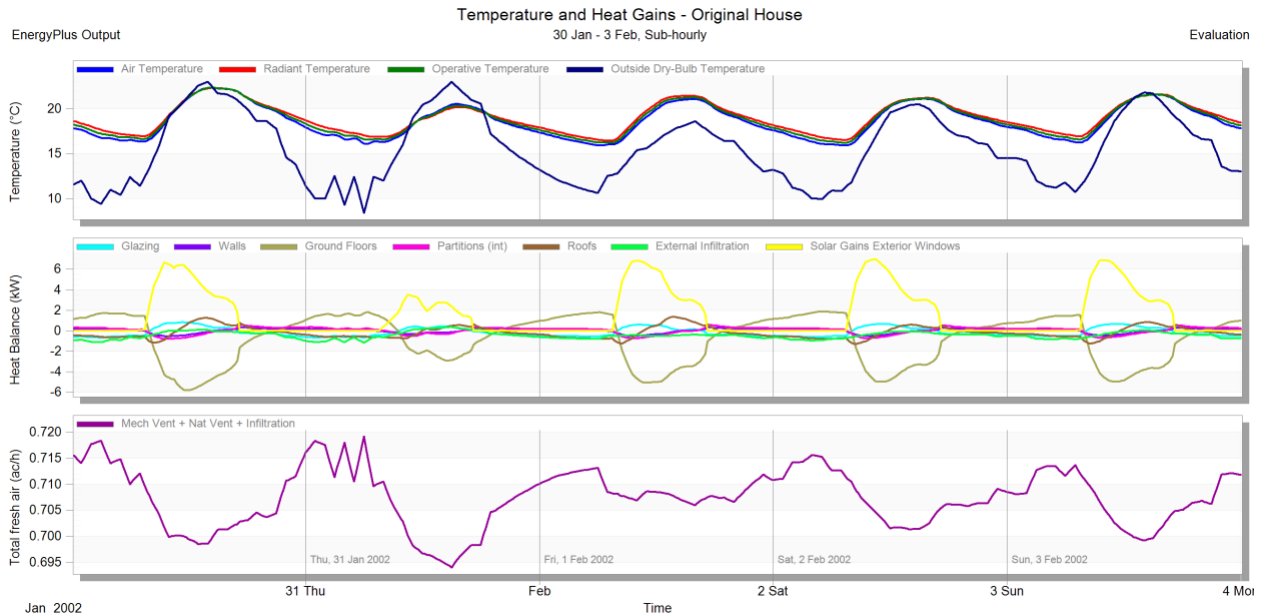


Figure 40: Graph for Original House Simulation $\times 10$ Wall Insulation Thickness

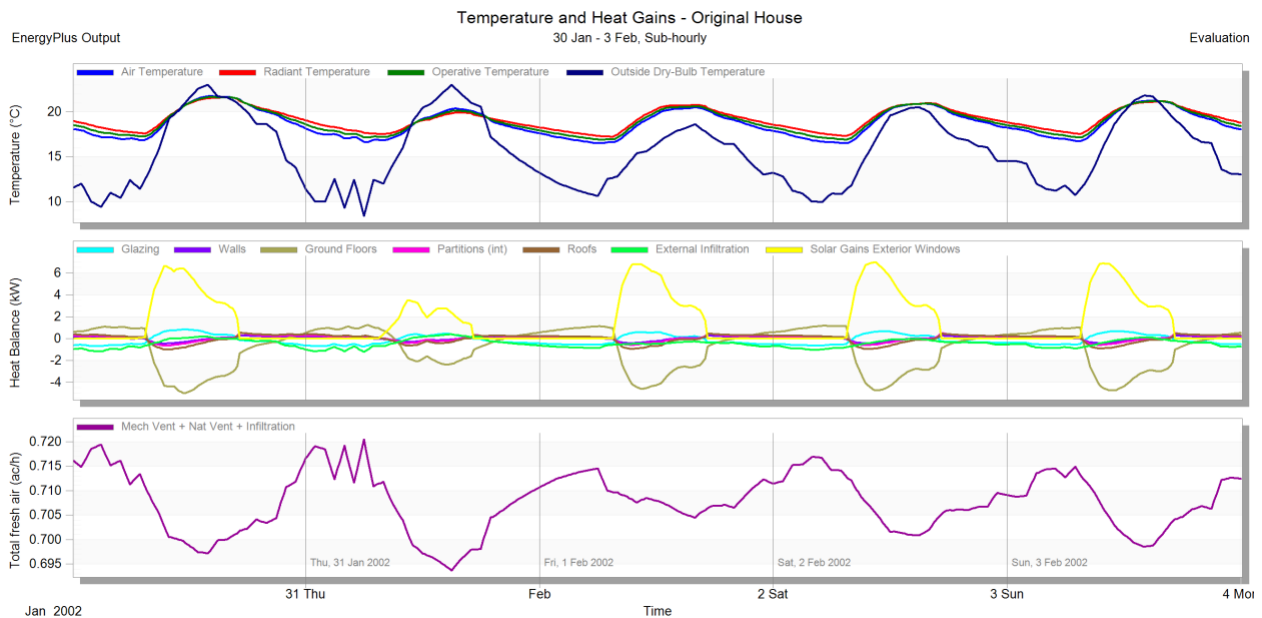


Figure 41: Graph for Original House Simulation Ceiling $\times 10$ and Wall $\times 10$ Thickness

Before moving on to other single changes, the two iterations of thicker wall insulation and thicker ceiling insulation were combined. The thermal behavior can be seen above in Figure 34. The result is an even more moderate temperature difference between night and day inside of the structure. One can see that the peak temperature is decreased by a few degrees across all five days, and the coolest temperature is around 17 or 18 centigrade depending on the type of temperature you are looking at.

Iteration 3: Heating System Timer

Season	Time (Hours)	Cost per kWh in agurot (shekel/100)		
		Sun - Thurs	Fri, Day before Holiday	Shabbat and Holiday
Summer (July-Aug)	07 to 10	40.4	27.16	27.16
	10 to 17	92.62	27.16	27.16
	17 to 21	40.4	27.16	27.16
	21 to 07	27.16	27.16	27.16
Winter (Dec-Feb)	06 to 08	49.86	29.67	29.67
	08 to 16	29.67	29.67	29.67
	16 to 17	83.73	49.86	29.67
	17 to 19	83.73	49.86	83.73
	19 to 20	83.73	49.86	49.86
	20 to 21	83.73	29.67	49.86
	21 to 22	83.73	29.67	29.67
Spring/Fall (Mar-July, Sept-Nov)	22 to 06	29.67	29.67	29.67
	06 to 17	39.74	32.4	26.37
	17 to 20	39.74	32.4	32.4
	20 to 21	32.4	26.37	32.4
	21 to 22	32.4	26.37	26.37
	22 to 06	26.37	26.37	26.37

Figure 42: Neot Semadar Electricity Costs by season, week day, hour, in agurot. 17% VAT not included

The third iteration included creating a simulation that incorporated a heating system that only went on at specific times. The times would be times where 1) electricity

costs are lower and 2) when the natural temperature during the winter would leave the comfort zone. The table in Figure 35, above, displays electricity costs in agurot per kWh (kilowatt-hours) for different seasons, days, and hours of the year.

This graph was created based off of two graphs, found in Appendices A and B, provided by the sponsor that were translated from Hebrew by Austin Shalit, a Hebrew-speaking IQP WPI student on-site. For the purposes of this iteration, the cost efficiency goal focused on the Sunday through Thursday electricity schedule, excluding Shabbat, and holidays, and during the winter season (December – February). This provides us with the following electricity costs schedule:

06 to 08 = 49.86 agurot per kWh

08 to 16 = 29.67 agurot per kWh

16 to 22 = 83.73 agurot per kWh

22 to 06 = 29.67 agurot per kWh

We can see from this schedule that it would be most cost efficient to run a heater between the hours of 22 to 06 (10PM- 6AM) and 08 to 16 (8AM – 4PM), and approximately double that cost for 06 to 08 (6AM to 8AM). The simulation was designed to run a heater on a schedule from 22 to 06 (10 PM – 6AM) and see if that would help keep the house in the comfort zone at night.

Unfortunately do to time constraints and technical difficulties, this iteration was inconclusive and did not yield a successful simulation. However, one can imagine that the effect of heating at night would lead to an overall increase temperature at those times, perhaps avoiding the passive solar heating zone altogether and keeping the house in or closer to the comfort zone day and night, while using the most cost-efficient electricity.

Iteration 4: Adjust Shading/Glazing

The fourth and final iteration was to adjust shading and glazing characteristics of the model to see how thermal behaviors changed throughout the simulation. This was done by adjusting the editing the openings tab for the original house construction. The default amount of shading for all other simulations was 30% for the original house. The two additional shading values that were tested were as follows:

- 1) 10 % - lower than default
- 2) 60% - higher than default

Figure 36 below, shows the panel that was edited in order to complete these iterations. The layout field was changed to the relevant percentages with the preferred height of the glazing remaining at 1.5m.

Glazing Template	
Template	Project glazing template
External Windows	
Glazing type	Project external glazing
Layout	Preferred height 1.5m, 30% glazed
Dimensions	
Type	3-Preferred height
Window to wall %	30.00
Window height (m)	1.50
Window spacing (m)	5.00
Sill height (m)	0.80
Outside reveal depth (m)	0.000
Frame and Dividers	
Shading	
<input checked="" type="checkbox"/> Window shading	
Type	Blind with high reflectivity slats
Position	1-Inside
Control type	15-Night heating + day cooling
Slat Angle Control	

Figure 43: Shading Properties for Original House Structure

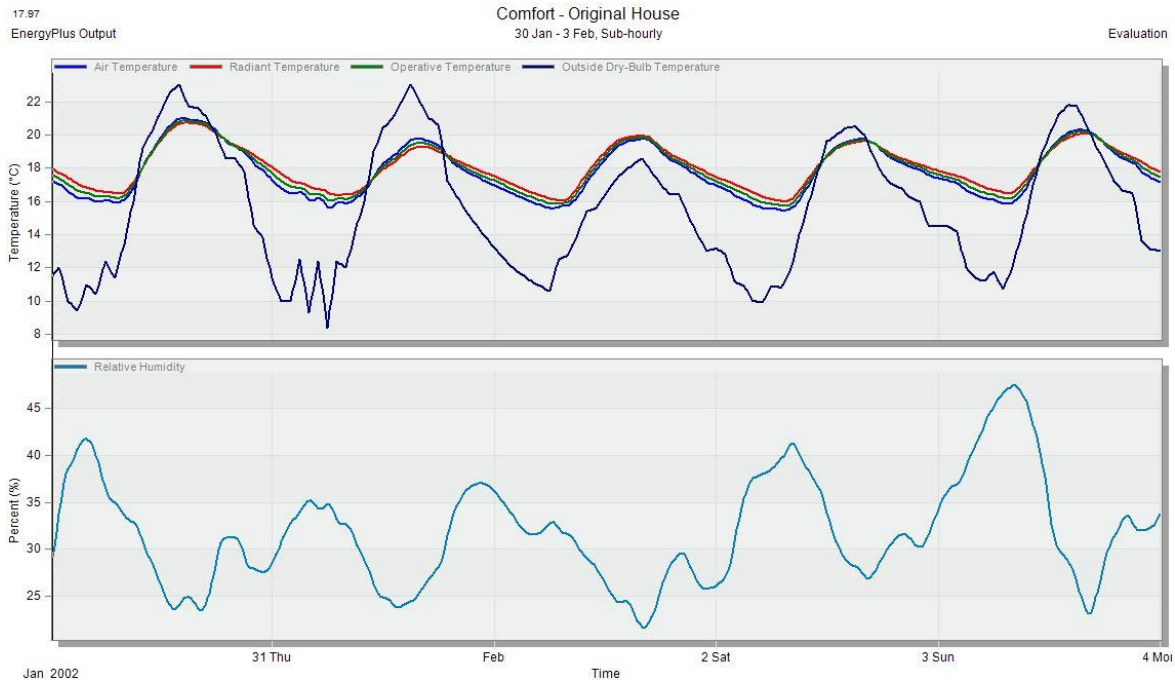


Figure 44: Winter Simulation with 10% glazing, comfort data

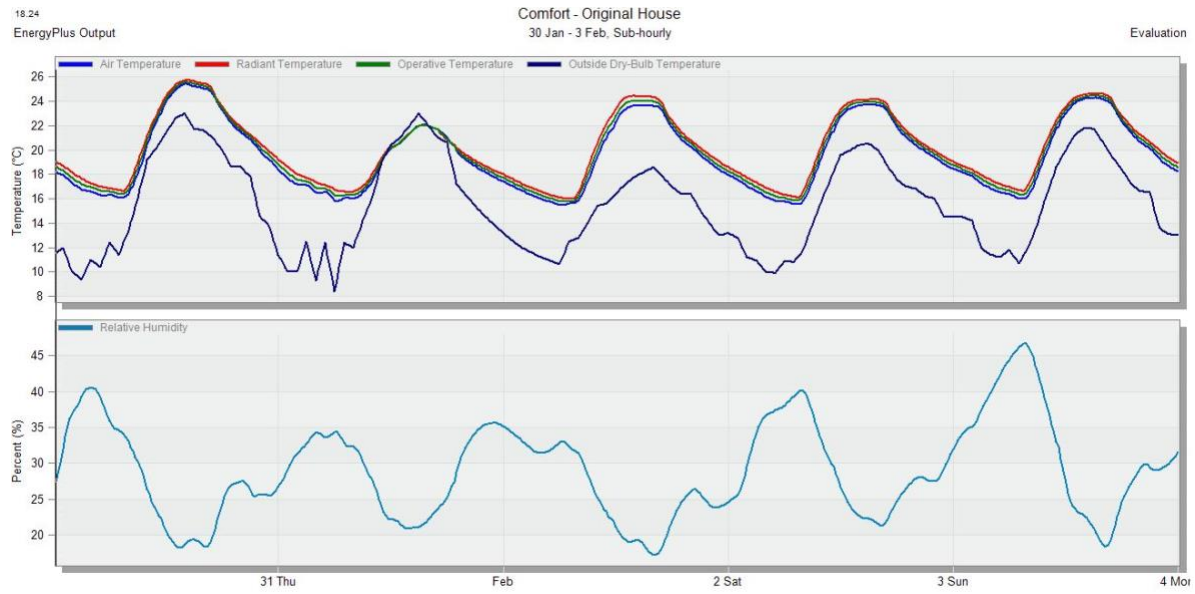


Figure 45: Winter Simulation with 60% glazing, comfort data

Figures 37 and 38 above, show the thermal behavior of the original housing structure with the variable glazing values. With less glazing, the peak temperature during the day is around 20-21 centigrade and remains lower than the outside dry-bulb temperature signifying that there is a high heat gain from glazing throughout the house. This is of course also evident in the non-changed simulation that displays the heat losses and gains. Figure 38 shows how drastic the effect from glazing can be in a home without natural ventilation, similarly to a car with the windows and doors shut on a sunny day.

Figure 39 shows the simulation data when glazing was returned to the default value of 30% and shading added to the environment. As seen in Figure 36, the shading was due to high reflectivity blinds on the inside of the external windows.

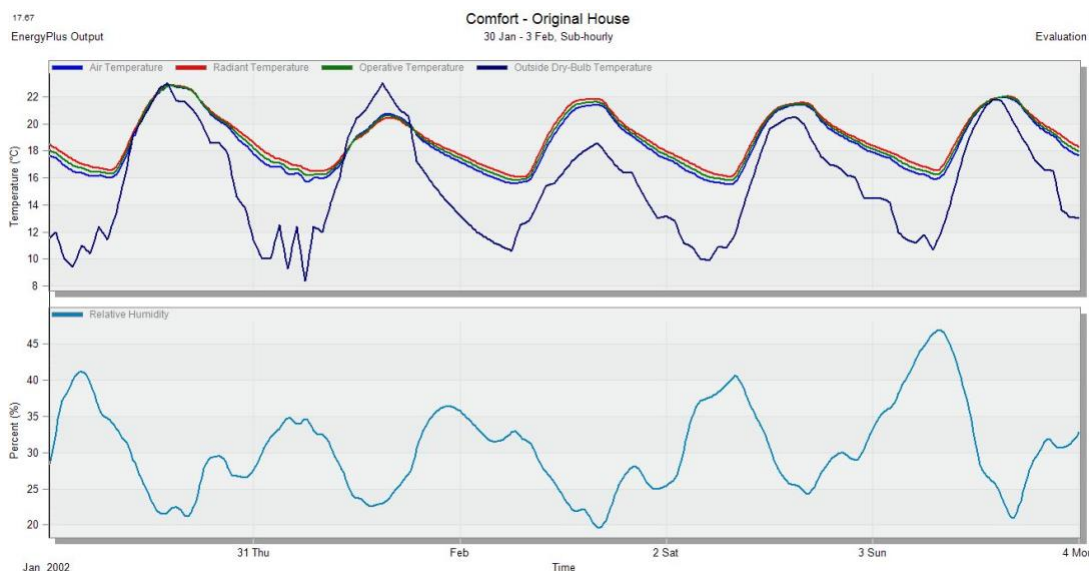


Figure 46: Winter Simulation with Shading

We can see that there is actually not much of a change to this data from the non-changed original house. Perhaps this is because the blinds are inside. The reason for

not repeating the simulation with external blinds is that covering the windows from the outside would effectively be reducing the glazing percentage.

6 On-Site Data Collection

In order to gain a thorough understanding of how current energy usage and temperature patterns manifest themselves in the kibbutz buildings during the time of the visit, data collection is imperative. The data that was collected by the IQP team mentioned in the introduction consisted of temperature values (dry bulb and wet bulb) at various heights inside of the houses, as well as inside the roof structure, and the outside temperature using a device created by the IQP team over the course of a month.

While on-site at Neot Semadar, the team constructed and tested the multi-sensor device that was placed in various types of houses throughout Neot Semadar. The purpose of creating these devices was to explore current conditions at Neot Semadar in an effort to compare performance of high thermal mass houses to houses with lighter construction and higher insulation. Leaving these devices with the sponsor also will allow them to continue temperature measurements in the summer-the more energy intensive season in terms of heating/cooling systems.

The data collected by these devices was useful for this project since they measured Iris' house as well as a house with higher thermal mass, amongst many others. It was interesting to see how heat was retained and lost within these houses during the time that data was collected. This enabled a comparative study between the theoretical and actual data. The device placed in Iris' house was fitted with the standard sensors and they each were placed at controlled heights.

Figure 40 below, shows the data that was collected inside of Iris' house and Figure 41 shows the data that was collected within a high thermal mass house

belonging to a woman named Israella. They can be found in appendices C and D for more visual clarity. The local weather data for outside dry-bulb temperature can be found in appendix E.

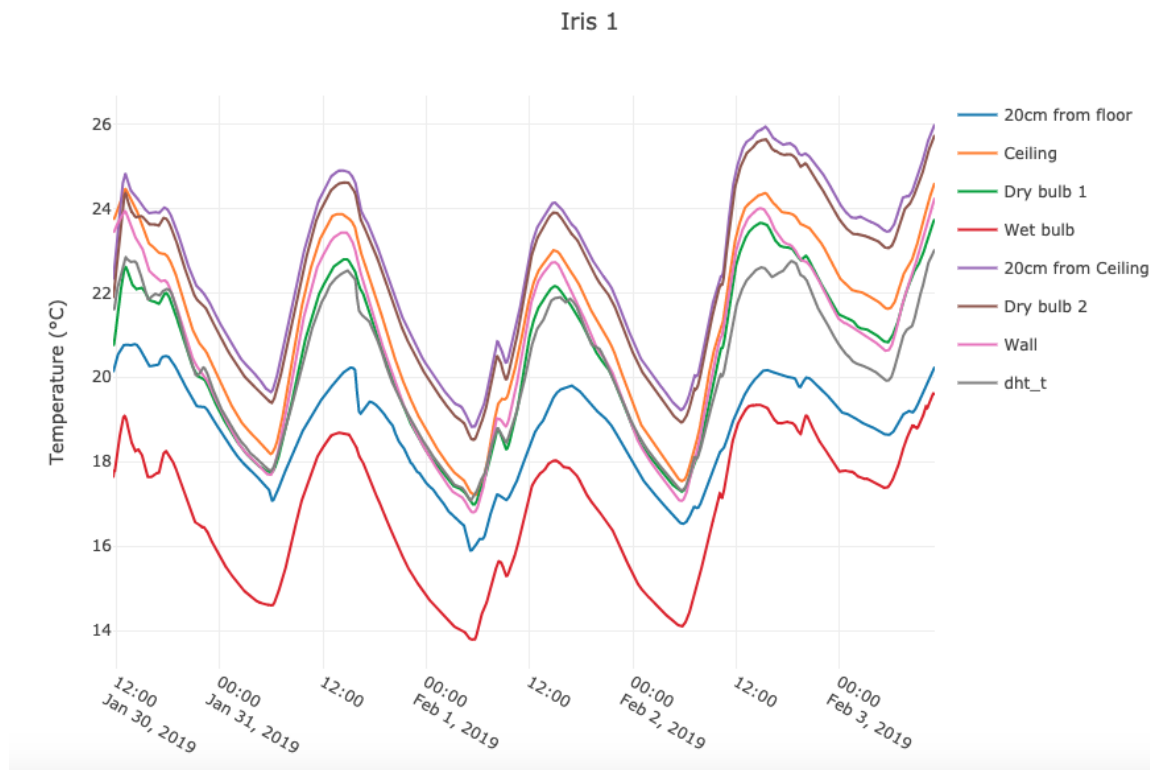


Figure 47: Real Data from Light-weight house, Iris', January 30th through February 3rd

In the five-day data set for Iris's house there are eight temperatures plotted in centigrade. The sensors are represented by Ceiling, 20cm from Ceiling, Wet Bulb, Dry bulb 1, Dry bulb 2, and Wall. The outside temperature is represented by dht_t. You can see that similarly to the simulation the peak temperature inside is higher than the outside peak temperature. The temperatures higher up in height in the house are

warmer, and the walls and floor were the coolest indoor temperatures. This shows the real-life phenomenon of the tiled ground of Iris' house acting as a heat sink. The wall temperature also shows that the heat within the house is not due to a radiation of heat off of the walls but due to the temperature of the air when the heater is on.

Figure 41 shows the data from Israella's house which was one of the first houses built by Neot Semadarian. It is high in thermal mass and is a key example of the type of design that the kibbutz previously strove for. One can see the same sensors listed to the right of the graph, with dht_t being the outside temperature.

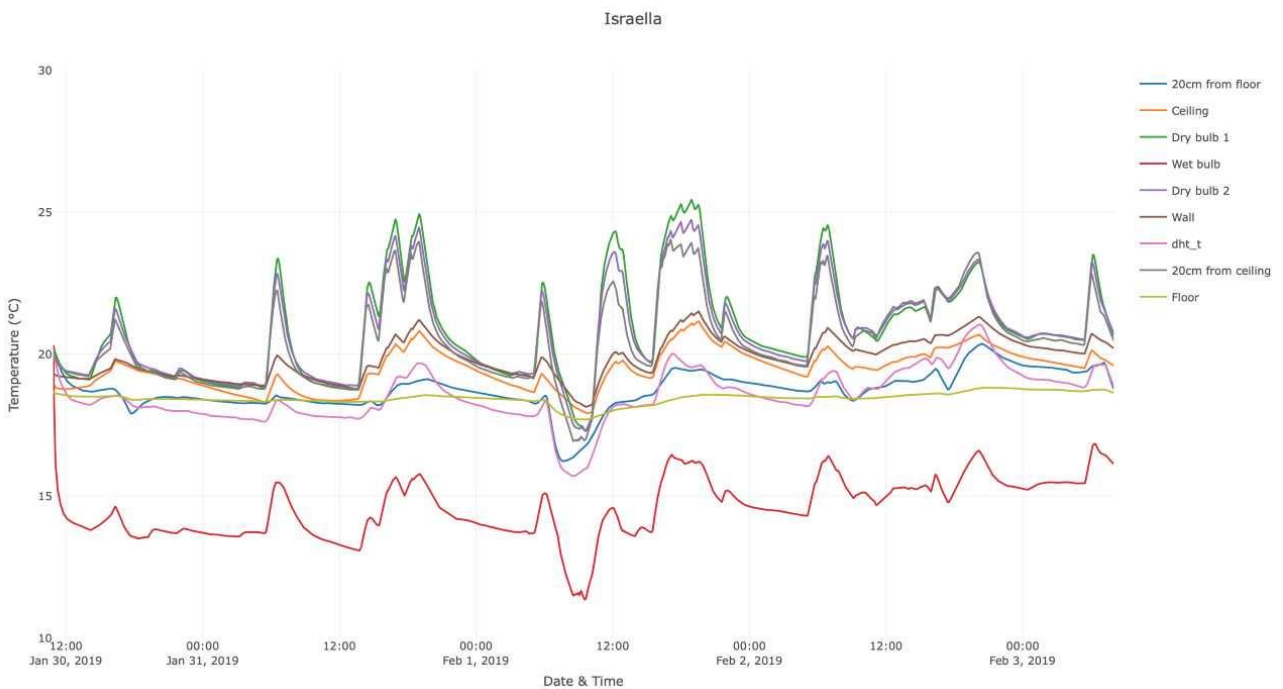


Figure 48: Real Data from High Thermal Mass house, Israella's, January 30th through February 3rd

In Israella's house, for the same five days of January 30th through February 3rd, one can see the difference in curve behavior for a high thermal mass structure. At first glance it might seem like when the outside temperature increases, there is a steep

increase in indoor temperatures and it is sustained at its peak, with a relatively high value, well beyond the peak outdoor temperature. While this is a valid property of a high thermal mass house, the sustained high temperatures are from a heater in the house that is oscillating on and off. One can notice however, that the house is very slow to cool down. This can be a major problem in the summer months, even if natural ventilation is an option. Unsurprisingly, the floor remains much cooler than the rest of the sensors inside.

This real data was helpful in understanding and explaining how much human behavior influences a home in terms of its energy use and daily temperatures within a structure.

8 Future Work and Challenges

In examining potential solutions to increase the comfort in housing year-round there was a significant anticipated challenge worth noting; the timing of the on-site project. The most challenging time of the year for Neot Semadar to remain both energy efficient and comfortable is during the summer months (April to October) which is characterized by hot and dry weather. This project took place from January to early March, which is considered their winter and is characterized by mild temperature and occasional rain showers.

There is high value to having real data during the summer and being able to work on solutions to Neot Semadar's unbearable heat. In order to bridge the gap between winter temperature data and the realities of the harsh hot summer, DesignBuilder software can be used by future students to model summer weather data for the given geometry of the houses at Neot Semadar, and the sensors that were left with the kibbutz can be employed. Models for each significantly different house could incorporate solar data for the specific coordinates and time of the year under examination. This could be studied alongside the project sponsor and shed light on potential areas from which further recommendations can be made.

9 Conclusion

This project provided theoretical and actual context for thermal behavior within a residential environment through a practical application to a specific house at Neot Semadar. Modeling this house along with collecting real temperature data sub-hourly for multiple days allowed this project to bridge the gap between theoretical and actual properties. It took into consideration bioclimatic architectural principles and best practices of mechanical engineering heat transfer analysis as well as open-mindedness and adaptation. Through a variety of methods this project drew helpful comparisons between high thermal mass houses and more light-weight and insulated houses, hopefully aiding the sponsor in their quest to find the perfect balance of housing envelope characteristics between the two styles.

References

- Singh, Manoj Kumar, Mahapatra, Sadhan, and Atreya, S.K. "Thermal Performance Study and Evaluation of Comfort Temperatures in Vernacular Buildings of North-East India." *Building and Environment* 45, no. 2 (2010): 320–329.
- Leichman, Abigail Klein, Marian Lebor, Sally Halon, and Viva Sarah Press. "The Taj Mahal of the Middle East." *Israel21c*. January 20, 2014.
- Manzano-Agugliaro, Francisco, Montoya, Francisco G., Sabio-Ortega, Andrés, and García-Cruz, Amós. "Review of Bioclimatic Architecture Strategies for Achieving Thermal Comfort." *Renewable and Sustainable Energy Reviews* 49, no. C (September 2015): 736–755.
- Gaitani N, Mihalakakou G, Santamouris M. On the use of bioclimatic architecture principles in order to improve thermal comfort conditions in outdoor spaces. *Build Environ* 2007;42(1):317–24. <http://dx.doi.org/10.1016/j.buildenv.2005.08.018> URL (<http://www.sciencedirect.com/science/article/pii/S0360132305003409>).
- weatheronline.co.uk. "Israel and Palestine." WeatherOnline, www.weatheronline.co.uk/reports/climate/Israel-and-Palestine.htm.
- Britannica, The Editors of Encyclopaedia. "Tropical and Subtropical Desert Climate." *Encyclopædia Britannica*, Encyclopædia Britannica, Inc., 14 Mar. 2016, www.britannica.com/science/tropical-and-subtropical-desert-climate#ref1092496.
- Huang, Yongping, et al. "A Method to Measure Humidity Based on Dry-Bulb and Wet-Bulb Temperatures." *Research Journal of Applied Sciences, Engineering and Technology*, vol. 6, no. 16, Sept. 2013, pp. 2984–87, doi:10.19026/rjaset.6.3682.
- Casella, Franco, et al. "Modeling the Dynamic and Thermodynamic Operation of Stirling Engines by Means of an Equivalent Electrical Circuit." *Energy Conversion and Management*, vol. 150, Elsevier Ltd, Oct. 2017, pp. 295–303, doi:10.1016/j.enconman.2017.08.027.
- Mesoclimate - Oxford Reference. (2017, June 16). Retrieved February 14, 2019, from <http://www.oxfordreference.com/view/10.1093/oi/authority.20110803100152176>
- Thermal Envelope - Low Energy Home: Building an energy efficient passive house. (n.d.). Retrieved March 23, 2019, from <https://sites.google.com/site/lowenergyhome/thermal-envelope>
- U. (n.d.). 2018 IECC Commercial Scope and Envelope Requirements. Retrieved from https://www.energycodes.gov/sites/default/files/becu/2018_IECC_commercial_requirements_envelope.pdf

Appendices

Appendix A: Regional Electricity Cost by Season, Week Day, Time Part 1

הגדרת שעות הצריכה ומחירי הקוט"ש



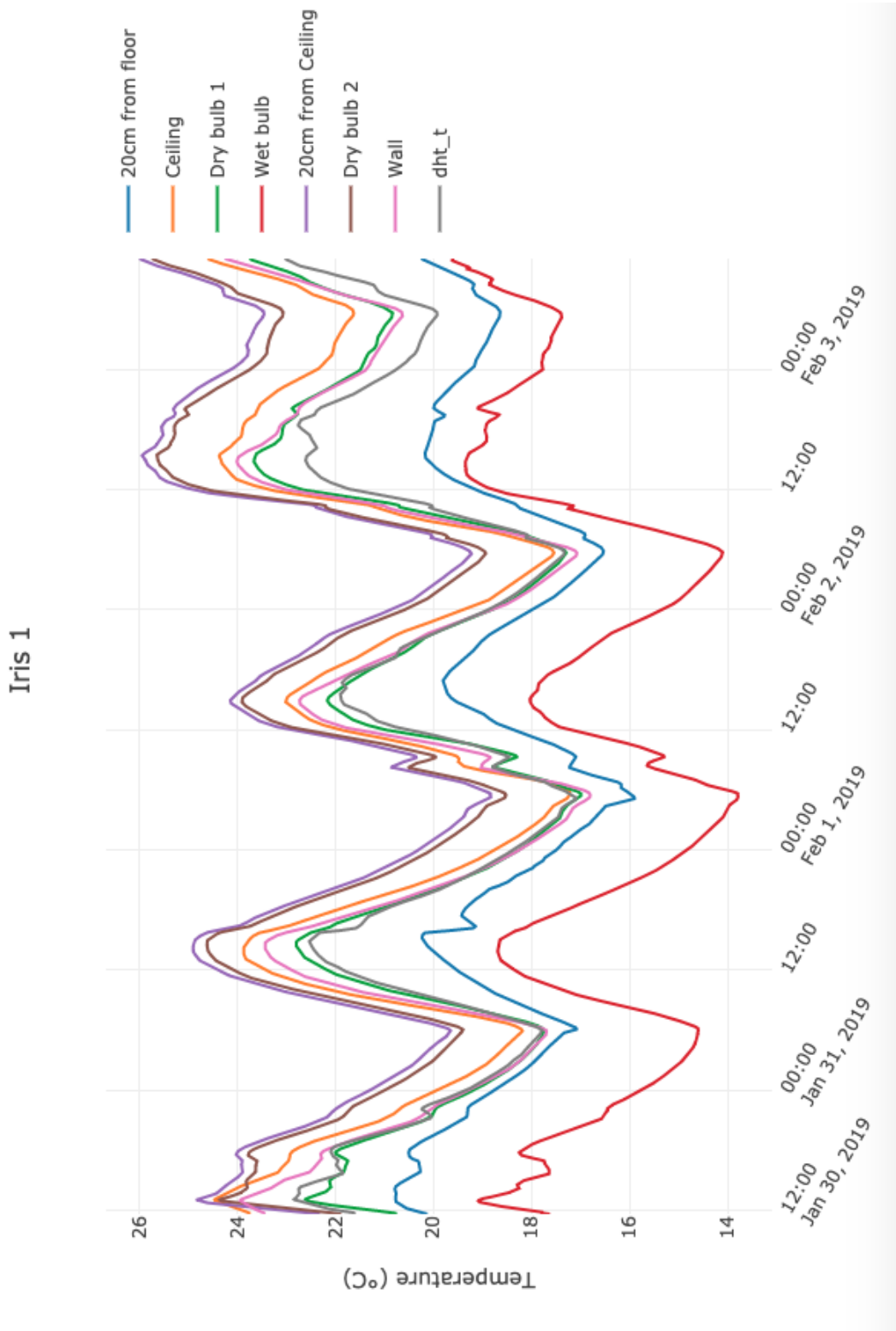
Appendix B: Regional Electricity Cost by Season, Week Day, Time Part 2

מחירי התעו"ז במתח גבוה

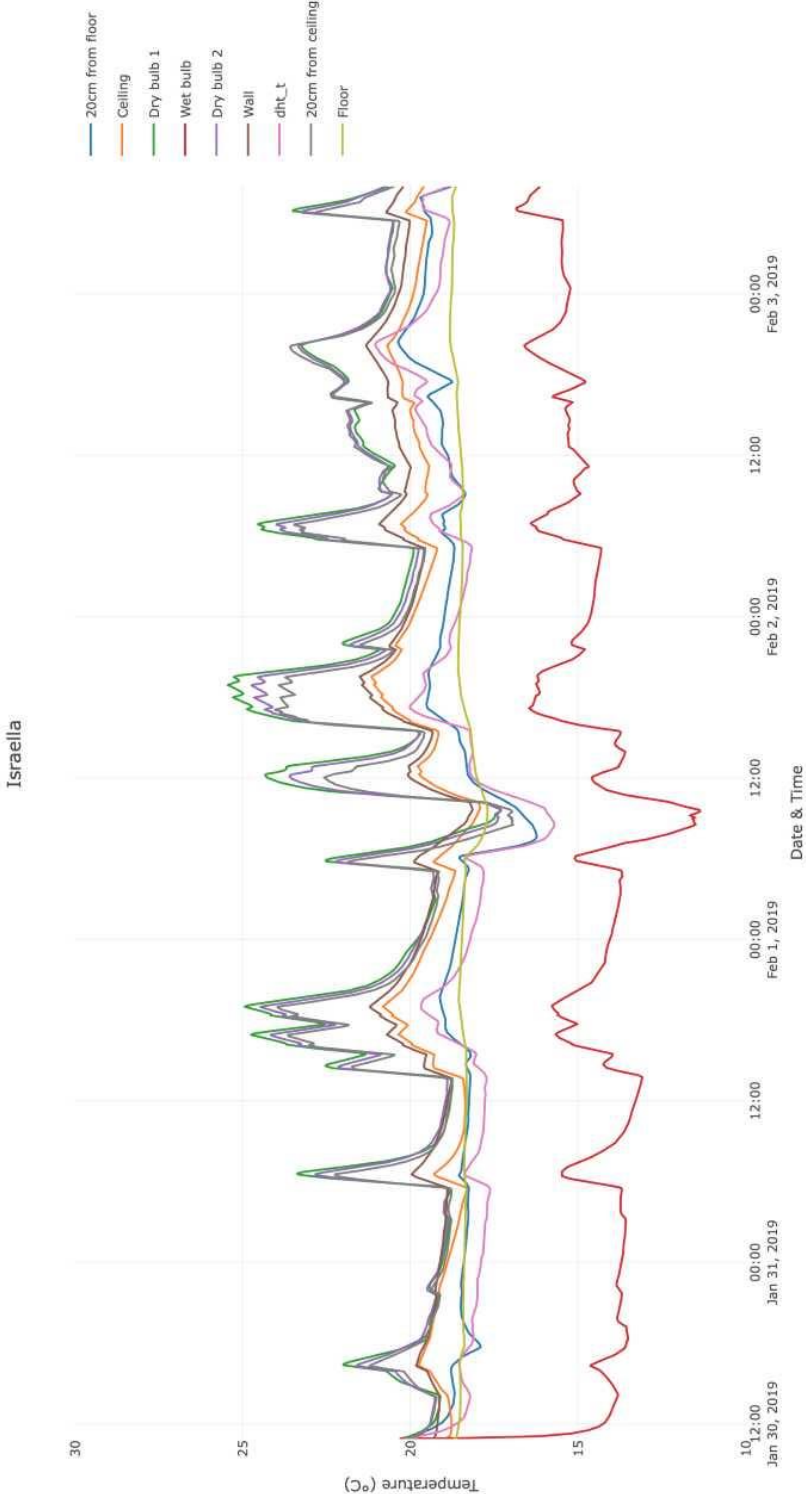
בתוקף מ - 01.01.2019

מחיר לקוט"ש באגרות כולל מע"מ	מחיר לקוט"ש באגרות לא כולל מע"מ	שעות הצריכה בשבתות ובחגים	שעות הצריכה בימי 'ו' ובערבי חג	שעות הצריכה בימים א'-ה'	מקבצי השעות	החודשים	העונה
110.88	94.77	אין	אין	משעה 10 עד 17	פסגה	יולי עד אוגוסט	קיץ
47.22	40.36	אין	אין	משעה 07 עד 10 ומשעה 17 עד 21	גבע	יולי עד אוגוסט	קיץ
31.27	26.73	משעה 00 עד 24	משעה 00 עד 24	משעה 00 עד 07 ומשעה 21 עד 24	שפל	יולי עד אוגוסט	קיץ
102	87.18	משעה 17 עד 19	אין	משעה 16 עד 22	פסגה	דצמבר עד פברואר	חורף
60.28	51.52	משעה 19 עד 21	משעה 16 עד 20	משעה 06 עד 08	גבע	דצמבר עד פברואר	חורף
34.77	29.72	משעה 00 עד 17 ומשעה 21 עד 24	משעה 00 עד 16 ומשעה 20 עד 24	משעה 00 עד 06 משעה 08 עד 16 ומשעה 22 עד 24	שפל	דצמבר עד פברואר	חורף
46.86	40.05	אין	אין	משעה 06 עד 20	פסגה	מארס עד יוני ספטמבר עד נובמבר	אביב/סתיו
37.86	32.36	משעה 17 עד 21	משעה 06 עד 20	משעה 20 עד 22	גבע	מארס עד יוני ספטמבר עד נובמבר	אביב/סתיו
30.68	26.22	משעה 00 עד 17 ומשעה 21 עד 24	משעה 00 עד 06 ומשעה 20 עד 24	משעה 00 עד 06 ומשעה 22 עד 24	שפל	מארס עד יוני ספטמבר עד נובמבר	אביב/סתיו

Appendix C: Real Data from Light-weight house, Iris', January 30th through February 3rd



Appendix D: Real Data from High Thermal Mass house, Israella's, January 30th through February 3rd



Appendix E: Neot Semadar Weather Station Data, January 30th through February 3rd

